

# Development of Inhibitory Circuitry in Visual and Auditory Cortex of Postnatal Ferrets: Immunocytochemical Localization of Calbindin- and Parvalbumin-Containing Neurons

WEN JUN GAO,<sup>1</sup> AMY B. WORMINGTON,<sup>2</sup> DOUGLAS E. NEWMAN,<sup>3</sup>  
AND SARAH L. PALLAS<sup>1\*</sup>

<sup>1</sup>Department of Biology, Georgia State University, Atlanta, Georgia 30302

<sup>2</sup>University of Pittsburgh School of Medicine, Pittsburgh, Pennsylvania 15261

<sup>3</sup>263 West End Avenue, New York, New York 10023

---

---

## ABSTRACT

The inhibitory neurotransmitter  $\gamma$ -aminobutyric acid (GABA) is thought to play an important role in activity-dependent stages of brain development. Previous studies have shown that different functional subclasses of cortical GABA-containing neurons can be distinguished by antibodies to the calcium-binding proteins parvalbumin and calbindin. Thus insight into the development of distinct subsets of inhibitory cortical circuits can be gained by studying the development of these calcium-binding protein-containing neurons. Previous studies in several mammalian species have suggested that calcium-binding proteins are upregulated in sensory cortex when thalamocortical afferents arrive. In ferrets, the ingrowth of thalamic axons into cortex occurs well into postnatal development, allowing access to early stages of cortical development and calcium-binding protein expression. We find in ferrets that both parvalbumin- and calbindin-immunoreactivity are present in primary visual and primary auditory cortex long before thalamocortical synapse formation, but that there is a sharp decline in immunoreactivity by postnatal day 20. Day 20 in ferrets corresponds to postnatal day 1 in cats, and thus previous studies in postnatal cats would have missed this early pattern of calcium-binding protein distribution. Another surprising finding is that the proportion of parvalbumin- and calbindin-immunoreactive neurons peaks secondarily late in development, between P60 and adulthood. This result suggests that the parvalbumin- and calbindin-containing subclasses of nonpyramidal neurons remain immature until late in the critical period for cortical plasticity, and that they are positioned to play an important role in experience-dependent modification of cortical circuits. *J. Comp. Neurol.* 422:140–157, 2000. © 2000 Wiley-Liss, Inc.

**Indexing terms:** postnatal development; cortical development; calcium-binding proteins; critical period; GABA; carnivore

---

---

The neurotransmitter  $\gamma$ -aminobutyric acid (GABA) plays an important role in shaping the response properties of sensory cortical neurons in adult animals (Sillito, 1975a,b; Berman et al., 1992; Crook and Eysel, 1992; Sato et al., 1995, 1996; Allison et al., 1996; Crook et al., 1996, 1997, 1998; Das and Gilbert, 1999) and may also subserve critical functions during early (Berninger et al., 1995; Behar et al., 1996; Antonopoulos et al., 1997) and late (Reiter and Stryker, 1988; Hendry and Carder, 1992; Rutherford et al., 1997; Hensch et al., 1998; Zheng and Knudsen, 1999) cortical development. Our goal is to un-

---

Grant sponsor: National Science Foundation; Grant number: IBN-9511430; Grant sponsor: Whitehall Foundation; Grant number: F93-28; Grant sponsor: Georgia Research Alliance; Grant sponsor: NIH.

Wen Jun Gao's current address is: Section of Neurobiology, Yale University School of Medicine, 333 Cedar St., New Haven, CT 06510.

\*Correspondence to: Sarah L. Pallas, Department of Biology, Georgia State University, P.O. Box 4010, Atlanta, GA 30302. E-mail spallas@gsu.edu

Received 14 July 1999; Revised 17 February 2000; Accepted 21 February 2000

derstand the role of GABA and GABA-containing neurons in the construction of sensory cortical circuitry during postnatal development. In a previous study (Gao et al., 1999), we showed that GABA-immunoreactive (-ir) nonpyramidal neurons were numerous in ferret primary visual (V1) and primary auditory (AI) cortex at birth but declined in both density (cells/mm<sup>2</sup>) and proportion (GABA-ir neurons/total neurons) by the third postnatal week, as cortex matured. However, this maturational pattern was interrupted by an unexpected surge in the proportion of GABA-ir neurons at postnatal day (P) 60. This occurred long after the cortical layers were in place, and near the close of the critical period for ocular dominance plasticity (Chapman et al., 1996; Ruthazer et al., 1999). One aim of this study was to characterize further the neurons involved in the late peak of GABA-ir neurons. We have hypothesized that GABA plays a special role late in cortical development as circuits are being fine-tuned and may operate through a different and more prolonged process of synaptic modification than other forms of plasticity (Gao et al., 1999). Recent reports have established an important role for inhibitory circuitry in activity-dependent synaptic plasticity using physiological methods (Hensch et al., 1998; Zheng and Knudsen, 1999), and it is thus of interest to characterize the circuit components using anatomical methods.

GABA-ir neurons are a heterogeneous group, morphologically, neurochemically, and functionally (van Brederode et al., 1990; Hendry and Jones, 1991; Hendry and Carder, 1992; Hogan et al., 1992; Cauli et al., 1997; Gonchar and Burkhalter, 1997) and can even include pyramidal neurons early in development (Gao et al., 1999). Thus an understanding of their developmental role requires a description of how the distribution of the different subclasses of GABA-ir neurons changes during development. Calcium-binding proteins such as parvalbumin (PV) and calbindin (CB) have been found in separate subclasses of GABA-ir neurons in adult primary sensory cortex of several species. PV is found mainly in basket and chandelier neurons, and CB is found primarily in bipolar and double bouquet neurons (Fairén et al., 1984; Hendry et al., 1989; Hendry and Jones, 1991), although numerous reports of PV- and CB-ir pyramidal neurons also exist (e.g., van Brederode et al., 1991; Hogan and Berman, 1993; Preuss and Kaas, 1996). We describe here the distribution of PV- and CB-ir neurons during postnatal development in ferret (*Mustela putorius furo*) primary sensory neocortex.

Previous studies in cats, a closely related carnivore, have suggested that the expression of calcium-binding proteins occurs late in postnatal development and is trig-

TABLE 1. Number of Brains Used at Each Postnatal Age

	Nissl <sup>1</sup>		PV		CB	
	V1	AI	V1	AI	V1	AI
P1	7	7	4	4	5	4
P7	7	7	4	4	4	5
P14	8	8	7	4	7	6
P20	8	10	4	4	4	6
P40	9	9	4	5	5	5
P60	6	6	4	5	4	5
Adult	8	8	5	4	4	4
Total	53	55	32	30	33	35

<sup>1</sup>Data from Gao et al. (1999).

gered by the onset of thalamocortical innervation (Hendrickson et al., 1991; Alcántara and Ferrer, 1994, 1995; Hogan and Berman, 1994). In this study, examination of the pattern of PV and CB expression prior to the period of thalamocortical synapse formation is possible due to the relative immaturity of ferret sensory cortex at birth (Luskin and Shatz, 1985a; Jackson et al., 1989). In addition, a further contribution of this study is the quantitative analysis of PV and CB distribution from early stages of development in two different sensory cortical areas. We find that the distribution of PV- and CB-containing neurons is still changing late in cortical development, raising the possibility that the circuits formed by these neurons can take part in late stages of experience-dependent developmental plasticity.

Some of these results have been presented previously in abstract form (Newman et al., 1996).

## MATERIALS AND METHODS

### Animals

Neonatal and juvenile pigmented ferrets used in this study were the offspring of timed pregnant ferrets obtained from Marshall Farms (North Rose, NY), and adults used were jills that were no longer rearing litters. Data were obtained from 57 ferrets in total (Table 1). Some of the brains used in this study were also used for other projects. Postnatal time points studied were days (P) 1, 7, 14, 20, 40, and 60, and adulthood. These times were chosen to fall at intervals before, during, and after the critical period for ocular dominance plasticity (Issa et al., 1999; Ruthazer et al., 1999). Adults were at least 120 days old. All animals were treated in accordance with institutional and NIH Guidelines for the Care and Use of Laboratory Animals.

### Tissue preparation

Animals were euthanized with an overdose of sodium pentobarbital (65 mg/kg, i.p.), and perfused through the heart with 0.1 M phosphate-buffered saline (PBS; pH 7.4) followed by 4% paraformaldehyde or in a few early cases 4% paraformaldehyde with 0.1–0.2% glutaraldehyde in 0.1 M phosphate buffer (PB; pH 7.4). More reliable and intense immunolabeling was obtained when glutaraldehyde was eliminated from the fixation solution. Brains were extracted from the skull, postfixed overnight with 4% paraformaldehyde and 30% sucrose in PB for 24 (adult tissue) to 48 hours (neonatal tissue), and then transferred into 30% sucrose in PB at 4°C. Coronal sections were cut frozen at alternating thicknesses of 50 and 30 μm and

### Abbreviations

AI	primary auditory cortex
CB	calbindin D-28k
CB-ir	calbindin D-28k-immunoreactive
CP	cortical plate
GABA	γ-amino-butyric acid
GABA-ir	GABA-immunoreactive
IZ	intermediate zone
P	postnatal day
PV	parvalbumin
PV-ir	parvalbumin-immunoreactive
SP	subplate
V1	primary visual cortex

collected in 0.1 M PB. At 160- $\mu\text{m}$  intervals, one set of 50- $\mu\text{m}$  sections was mounted on gelatin-subbed slides and stained for Nissl substance with cresylecht violet. The other sets were used for immunocytochemistry.

### Immunocytochemistry

Visual and auditory cortex were identified based on their position (Kelly et al., 1986) and cytoarchitecture (Rose, 1949; Berman and Jones, 1982), as were the layers within each area. Sections from comparable brain regions and anterior-posterior (A-P) levels were processed for immunocytochemistry using standard avidin-biotin techniques. Most sections used for immunocytochemistry were 30  $\mu\text{m}$  in thickness, although in a few cases 50- $\mu\text{m}$  sections were used (AI: PV, 4 sections; CB, 2 sections; V1: PV, 4 sections; CB, 3 sections). The antibody penetrated to the same incomplete extent in 30- and 50- $\mu\text{m}$  sections, and thus the data were combined. All steps were performed under constant agitation.

Sections were first rinsed in 0.1 M PBS with 0.02% sodium azide and 0.3% Triton X-100, followed by 0.34% L-lysine and 0.05% sodium periodate ( $\text{NaIO}_4$ ) in PBS/azide/Triton for 1 hour to reduce free aldehydes. Nonspecific binding was suppressed by preincubation with 3% normal goat serum (NGS) in 0.1 M PBS with azide/Triton for 1 hour at room temperature. Sections were then transferred into primary antibody (parvalbumin: mouse anti-PV, 1:1000 or calbindin D-28k: mouse anti-CB, 1:200; both from Swant, Bellinzona, Switzerland) (Celio et al., 1988, 1990) in PBS with azide/Triton and 3% NGS, and incubated at 4°C for 48–72 hours. Titers of antibodies were high in order to bias against understaining, resulting in some background artifact, which was excluded from analysis. After thorough rinsing, biotinylated goat anti-mouse IgG at a dilution of 1:200 was used as the secondary antibody (incubation for 2 hours at room temperature). The secondary antibodies were visualized by incubation in avidin-biotin-peroxidase complex (ABC; Vectastain ABC Elite Kit, Vector, Burlingame, CA) for 60–90 minutes at a dilution of 1:500. The peroxidase complex was revealed by incubating the sections with 0.01% diaminobenzidine (DAB) and 0.004% hydrogen peroxide to which was added 1% nickel ammonium sulfate and 0.34% imidazole for intensification of the reaction product (Tago et al., 1989).

There are certain considerations to be taken into account in any immunocytochemistry experiment, such as the specificity of the antibodies. The antibodies used in this study have been well characterized (Celio et al., 1988, 1990) and have been employed in numerous studies in several different species. We demonstrated the specificity of the secondary antibody by preblocking with serum and by including primary antibody-free controls in each experiment. We never observed any immunoreactivity in these control sections. The specificity of the staining was further evidenced by the fact that only certain cell types showed immunolabeling with each of the two antibodies.

### Data analysis

Between four and seven animals were used for quantitative analysis at each developmental age (Table 1). For analysis of PV-ir neurons, 32 sections in V1 from 32 animals and 33 sections in AI from 30 animals were compared. For CB-ir neurons, 34 sections in V1 from 33 animals and 35 sections in AI from 35 animals were examined (Table 1). More than one section per brain re-

gion was analyzed quantitatively only in three cases where it was not clear that complete labeling had been obtained. Data from a previous study of Nissl-stained neurons, discussed here for comparison, included a total of 70 sections from the V1 of 53 ferrets, and 67 sections from AI of 55 ferrets (Gao et al., 1999). Immunocytochemistry was used to examine the emergence, distribution, and morphology of PV- and CB-ir neurons in V1 and AI of ferrets.

The neuronal morphology and areal and laminar distribution of both PV-ir and CB-ir neurons were qualitatively observed in cortical areas V1 and AI from each age group. For quantitative analysis, both Nissl- and adjacent antibody-labeled sections were used. Some of the Nissl-stained sections used in this study were also used in a previous study (Gao et al., 1999). For counts of Nissl-stained neurons, only neurons that contained clear, smooth, round or oval borders were counted. In some brains, more than one section was used from an area, and in this case the data were averaged. Care was taken to employ procedures that avoided double counts of neurons (Pallas et al., 1988; Gao et al., 1999). Neuronal diameter was used to correct for split cells according to the Abercrombie method, yielding data appropriate for relative comparisons between populations, and not absolute cell counts (Abercrombie, 1946; Guillery and Herrup, 1997). Estimates of neuron number were obtained within a 50- $\mu\text{m}$ -wide vertical strip across all cortical layers, using a 63 $\times$  or 100 $\times$  oil immersion objective and NeuroLucida software (MicroBrightfield, Colchester, VT). Strip area and neuronal number, proportion, and density within each strip were measured with the aid of Neuromorph software (MicroBrightfield).

For soma size measurements, the contours of both Nissl- and immunostained neurons were drawn under a 100 $\times$  oil-immersion lens using the NeuroLucida software, and areas and diameters were calculated and averaged by means of the Neuromorph software. The data were transferred into a Macintosh computer, and soma areas were categorized by their region, immunostaining, and postnatal age. Scheffe's ANOVA analyses were used for calculations of the mean, *F* value, and *P* value (Sokal and Rohlf, 1995). The comparisons are expressed as means  $\pm$  standard error (Table 2). Photomicrographs were prepared in Adobe Photoshop.

## RESULTS

Results obtained from a qualitative analysis of the distribution and morphology of PV- and CB-immunopositive neurons are presented here first, followed by a quantitative analysis of their density and proportion.

### Ontogeny of cortical cytoarchitecture

The cytoarchitectonic development of ferret sensory cortex (V1 and AI) as observed in this study followed the well-described inside-out (Rakic, 1974; McConnell, 1985) and rostrocaudal (Luskin and Shatz, 1985a) gradients of cerebral cortical development. In addition, there was some limited evidence for a rostrocaudal gradient, in that AI matured slightly earlier than V1. On the first day after birth (P1), which is approximately equivalent to embryonic day 42 (E42) in cats, the cortical plate had just formed (Jackson et al., 1989), and thus the cortical layers could not be identified. In this study, as in the previous one (Gao et al., 1999), we observed that the subplate (SP) was very thick at this stage (Fig. 1A,B). By P7, layer 6 appeared, as did layer 5 with its large neuronal cell bodies and relatively sparsely distributed

TABLE 2. Somatic area ( $\mu\text{m}^2$ ) of Nissl-Stained and PV- and CB-ir Neurons at Different Postnatal Ages (Analyzed by ANOVA).<sup>1,2</sup>

Age	V1 Nissl <sup>3</sup>	AI Nissl <sup>3</sup>	VI PV-ir	AI PV-ir	V1 CB-ir	AI CB-ir
P1	18.8 ± 0.51	20.2 ± 0.46	36.2 ± 1.40	36.1 ± 1.30	37.2 ± 1.47	46.4 ± 1.47
P7	21.3 ± 0.79	21.5 ± 0.64	46.7 ± 1.60	46.8 ± 2.31	35.7 ± 1.00	35.6 ± 1.13
P14	55.8 ± 2.27	61.6 ± 1.87	55.2 ± 2.50	48.6 ± 3.48	34.6 ± 1.65	67.0 ± 8.24
P20	40.9 ± 1.21	79.0 ± 3.49	32.1 ± 2.83	91.1 ± 9.23	56.8 ± 3.35	66.4 ± 3.48
P40	76.8 ± 3.91	124.1 ± 8.66	64.1 ± 5.12	50.2 ± 2.67	77.3 ± 5.08	64.3 ± 3.31
P60	100.3 ± 6.38	114.7 ± 8.69	93.7 ± 4.71	126.1 ± 7.80	91.2 ± 4.81	87.3 ± 5.50
Adult	60.3 ± 3.83	84.6 ± 2.10	59.4 ± 2.76	55.7 ± 3.75	59.4 ± 2.76	55.7 ± 3.75

<sup>1</sup>Probabilities that V1 and AI neurons are different sizes: *Nissl*: P1  $P = 0.05$ ; P7  $P = 0.84$ ; P14  $P = 0.07$ ; P20  $P < 0.0001$ ; P40  $P < 0.0001$ ; P60  $P = 0.02$ ; Adult  $P < 0.0001$ . *PV*: P1  $P = 0.93$ ; P7  $P = 0.26$ ; P14  $P = 0.14$ ; P20  $P = < 0.0001$ ; P40  $P = 0.01$ ; P60  $P < 0.0003$ ; Adult  $P < 0.43$ . *CB*: P1  $P < 0.0001$ ; P7  $P = 0.96$ ; P14  $P = 0.002$ ; P20  $P = 0.06$ ; P40  $P = 0.03$ ; P60  $P = 0.61$ ; Adult  $P = 0.43$ .  
<sup>2</sup>Probabilities that PV-ir and CB-ir somata are different sizes: *VI*: P1  $P = 0.62$ ; P7  $P < 0.0001$ ; P14  $P < 0.0001$ ; P20  $P < 0.001$ ; P40  $P = 0.08$ ; P60  $P = 0.72$ ; Adult  $P = 0.69$ . *AI*: P1  $P < 0.0001$ ; P7  $P < 0.0001$ ; P14  $P = 0.17$ ; P20  $P = 0.03$ ; P40  $P = 0.012$ ; P60  $P < 0.001$ ; Adult  $P = 0.96$ .  
<sup>3</sup>Data from Gao et al. (1999).

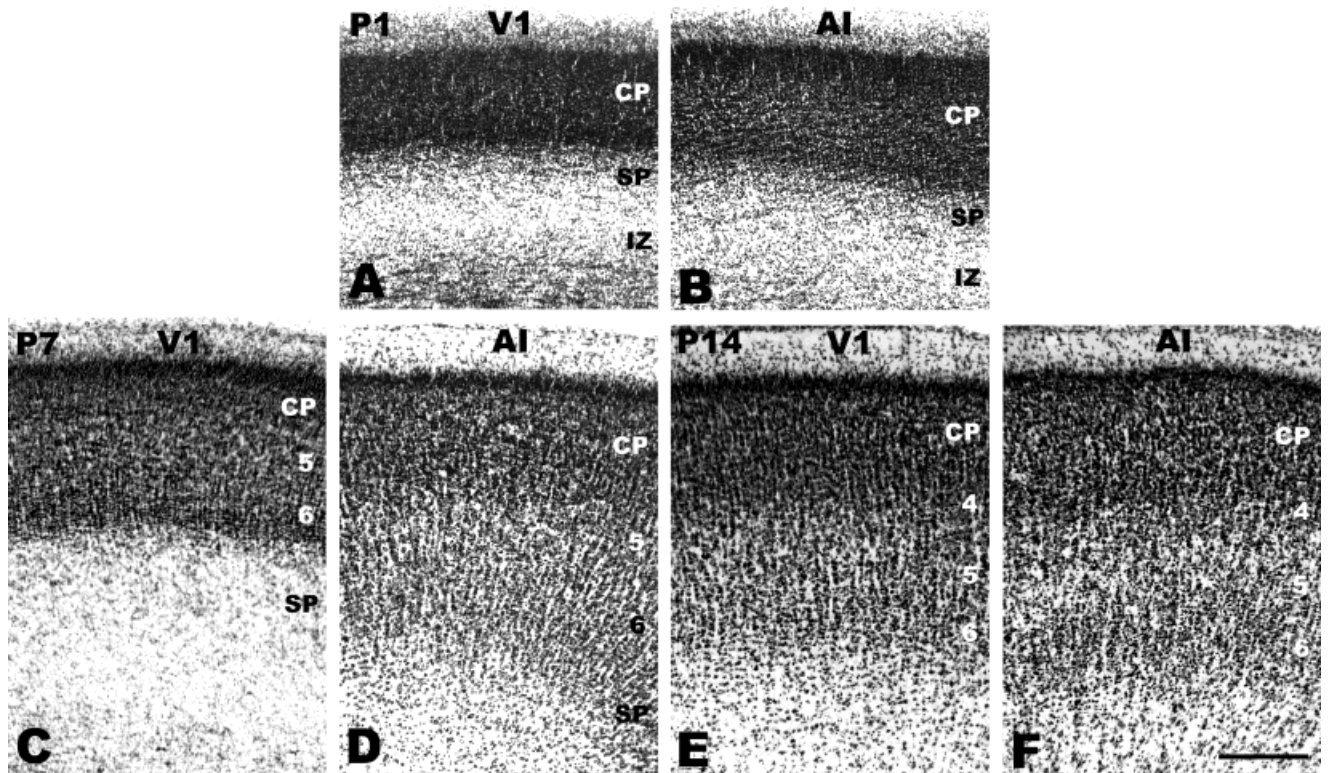


Fig. 1. Photomicrographs of Nissl-stained sections showing the early development of both visual (V1) and auditory cortex (AI) in ferrets. On the first day after birth (P1, **A,B**), the cortical plate (CP) and intermediate zones (IZ) were clearly distinguishable. The thick

subplate (SP) lay between these two strata. The marginal zone was located just below the pial surface. By P7 (**C,D**), layers 5 and 6 had formed and could be identified easily in both V1 and AI. At P14 (**E,F**), layer 4 could also be observed, especially in AI. Scale bar = 200  $\mu\text{m}$ .

neurons (Fig. 1C,D). As a more rostral area, AI matures earlier than V1, and this is reflected in the more well-differentiated layer 5 in AI at P7 (Fig. 1C,D). By P14, layer 4 had differentiated from the cortical plate (Fig. 1E,F), especially in AI. By P20, all the cortical layers could be identified, and the cortex had become thicker, but the total thickness of cortex was still less than in adulthood (Fig. 2A,B). By P40, the cortical structure was generally similar to that at P60 and adulthood, although neuronal density declined in the older animals, whereas soma size increased (Fig. 2C-H).

**Laminar distribution of PV-ir-neurons**

PV-ir neurons were widespread early in development, and then narrowed their distribution in late postnatal

stages, followed by a less restricted pattern again in adulthood. Numerous PV-ir neurons were found in the marginal zone, cortical plate, and subplate of V1 and AI at birth (Fig. 3A,B). At P7, although layers 5 and 6 had formed, they contained few neurons expressing PV, and the immunolabeled cells were mainly found in the subplate and at the top (in V1) or bottom (in AI) of the cortical plate (Fig. 3C,D). After the first postnatal week, PV immunoreactivity in terms of the number of immunostained cells and the intensity of their staining sharply decreased and declined to its lowest level by P20 (Figs. 3E,F, 4A,B), although dendritic and axonal staining increased at this stage. The PV-ir somata were located almost exclusively in layers 5 and 6 at P14 and P20. PV was also heavily

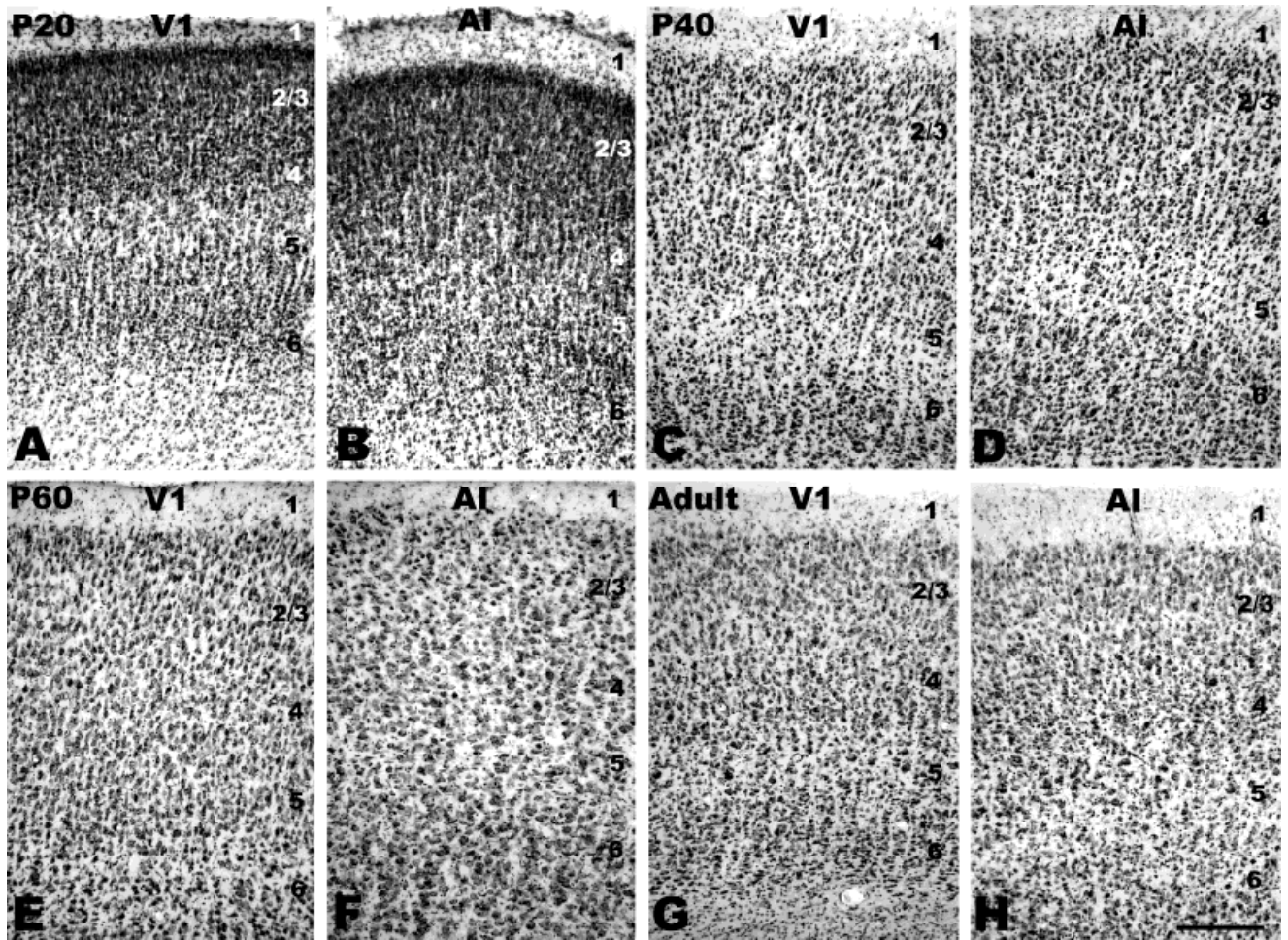


Fig. 2. Nissl staining of ferret neocortex at late stages of cortical development in V1 (A,C,E,G) and AI (B,D,F,H). All cortical layers could be identified by P20, and by P40, layers were becoming more easily distinguishable. By P60 (E,F), the cortical organization was generally similar to that in adulthood (G,H). Scale bar = 200  $\mu$ m.

expressed within the dendritic and axonal processes of the labeled neurons at P20. Thereafter, PV-ir neurons increased in quantity and were distributed in all cortical layers except layer 1 (Fig. 4C–H).

#### Laminar distribution of CB D-28k-immunoreactive neurons

In comparison with the wide laminar distribution of PV-ir neurons in adults, the CB-ir neurons in adults were arranged in a bilaminar fashion, in superficial and deep layers but not in the granular layer. On the day of birth, however, this bilaminar organization was not yet apparent. The cortical neurons that expressed CB were located mainly in the cortical plate and subplate on P1 (Fig. 5A,B) and were found throughout the CP, SP, and nascent layers 5 and 6 on P7 (Fig. 5C,D). Labeling was heaviest in the subplate. Fewer labeled neurons were observed in the cortical plate at P7 (Fig. 5C,D) than at P1, especially in V1. By P14, the number of CB-ir neurons had declined sharply in both V1 and AI. At this age, only a few neurons in the deep layers were immunoreactive to CB (Fig. 5E,F).

At P20 the situation was similar, in that the CB-ir neurons could be observed only at the bottom of layer 5 and in layer 6 (Fig. 6A,B), but there was some axonal staining, which was not commonly observed prior to this stage. During the following weeks, the number and intensity of immunoreactive neurons increased slightly, especially in layers 2/3, and became bilaminar at P40 (Fig. 6C,D), with labeled neurons mainly in layers 2/3 and 5/6 but not layer 4. At P60, however, there was a transient increase in CB-immunoreactivity in the middle layers, obscuring the bilaminar appearance (Fig. 6E,F). By adulthood, the distribution of CB-ir neurons was again bilaminar, in layer 2/3 and layers 5 and 6, with very few labeled neurons in lower layer 3 and layer 4 (Fig. 6G,H).

#### Morphological development of PV-ir neurons

We defined pyramidal neurons as those with a triangle-shaped soma and a thick apical dendrite, whereas migrating neurons have a bipolar, fusiform soma and leading and trailing processes of equivalent thickness (Peters and Jones, 1984). Nonpyramidal neurons were defined as

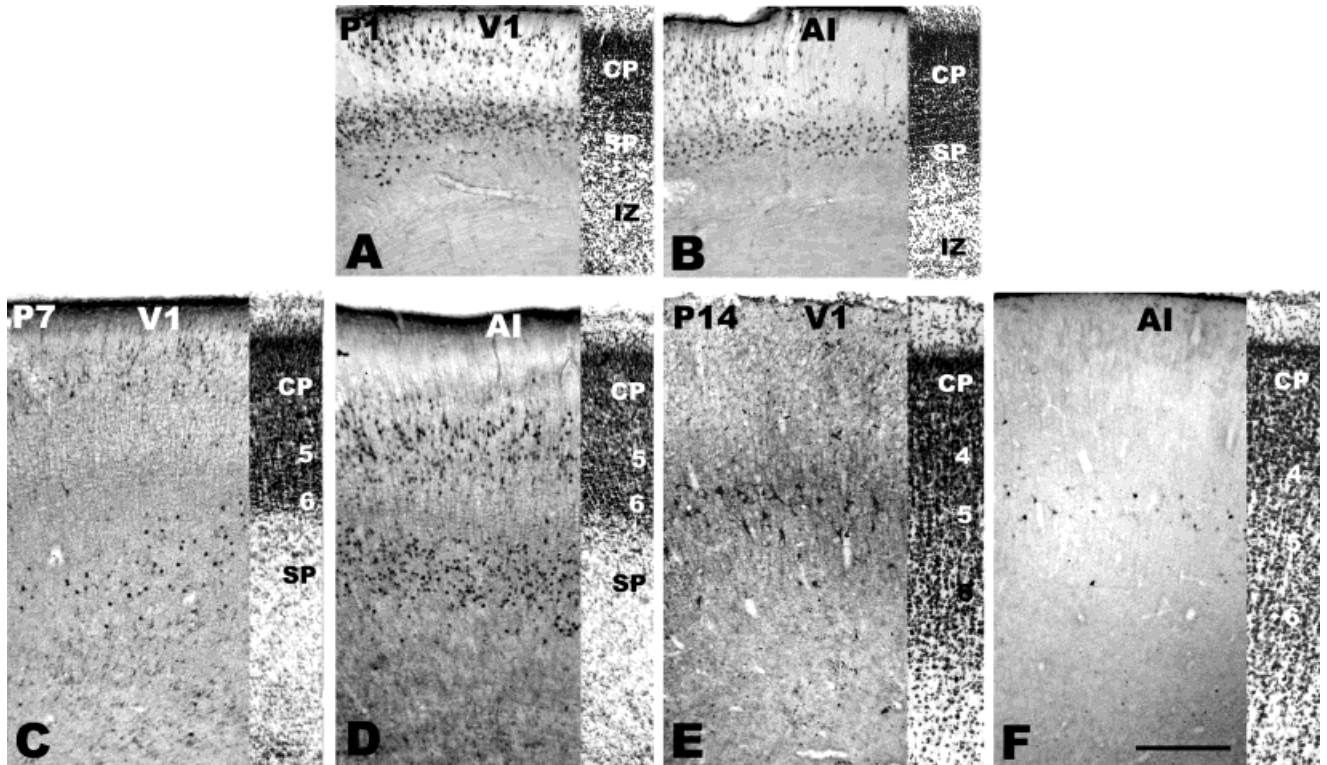


Fig. 3. Photomicrographs showing the early postnatal development of parvalbumin immunoreactive (PV-ir) neurons in both V1 (A,C,E) and AI (B,D,F). The PV-ir neurons were distributed in the marginal zone, cortical plate, and subplate at P1 (A,B) and included pyramidal as well as nonpyramidal neurons. There were fewer parvalbumin-positive neurons in the deep part of the cortical plate. By P7 (C,D), layers 5 and 6 were present but contained few PV-ir positive

neurons, as seen also in layer 1. By P14 (E,F), PV-ir neuronal number sharply decreased, owing partly to a loss of staining in the pyramidal neurons. Distributions of the immunostained neurons were also altered. There were very few if any PV-ir neurons in either the cortical plate (CP) or the subplate (SP) at P14. Instead, they could be found in layer 5 and occasionally in layer 6. Scale bar = 200  $\mu$ m.

those that did not fit in the other two categories. During the first postnatal week (P1, P7), the majority of PV-ir cells in the cortical plate were bipolar or pyramidal in shape, and only a few scattered, poorly differentiated cells resembled nonpyramidal neurons (Figs. 3A,B, 7A,B,E,F). In a previous study of GABA-ir neurons, GABA was also transiently observed in pyramidal neurons (Gao et al., 1999), although we have not yet examined whether both existed in the same pyramidal neurons. The vertically oriented bipolar neurons were probably migrating neurons and disappeared at later stages. Our methods cannot distinguish whether these neurons were changing their morphology, dying, or ceasing PV expression. The intensity and number of immunostained pyramidal neurons increased from P1 to P7, but they completely disappeared from the cortical plate by P14 (Fig. 3), suggesting that the expression of PV in cortical pyramidal neurons was a transient phenomenon.

In the subplate at P1 and P7, the PV-ir neurons were tadpole-shaped, with a round cell body and randomly oriented, short, tail-like dendrites (Fig. 7C,D). In the marginal zone subjacent to the pia, horizontally oriented cells with thick dendrites were observed that labeled with the antibody to PV (arrowheads in Fig. 7A,B). These were probably Cajal-Retzius cells and were observed only during the first postnatal week; they later disappeared or perhaps no longer expressed PV. At P14, PV-ir neurons

with complex morphology began to appear (Fig. 7G,H), and at P20, extensive dendritic and axonal staining were obtained, allowing a glimpse of the early widespread dendritic ramifications of this subclass of nonpyramidal neurons (Figs. 4A,B, 8A,B). By P40, PV-ir neurons often resembled their adult form (Figs. 4C,D, 8C,D), and little change in PV-ir neuronal morphology was observed between P40 and adulthood (Fig. 8C-H). The PV-ir neurons were diverse in form and included cells with small, medium, and large somata, with a multipolar morphology, including neurons resembling those described by others as chandelier or basket cells (Jones and Hendry, 1984; Peters, 1984).

### Morphological development of CB-ir neurons

At P1 and P7, most of the CB-ir neurons in the cortical plate were bipolar or pyramidal in shape and had strong immunoreactivity in their somata and apical dendrites (Figs. 5A-D, 9A-F). The vertically oriented bipolar neurons resembled migrating neurons and were not present at later ages. A small number of horizontally oriented, putative Cajal-Retzius cells were CB-ir. By P14, very few neurons in layers 5 and 6 expressed CB (Fig. 5E,F), and CB-ir pyramidal neurons were no longer observed. However, although the number of PV- and CB-ir neurons was decreasing, the neuronal processes, including dendrites

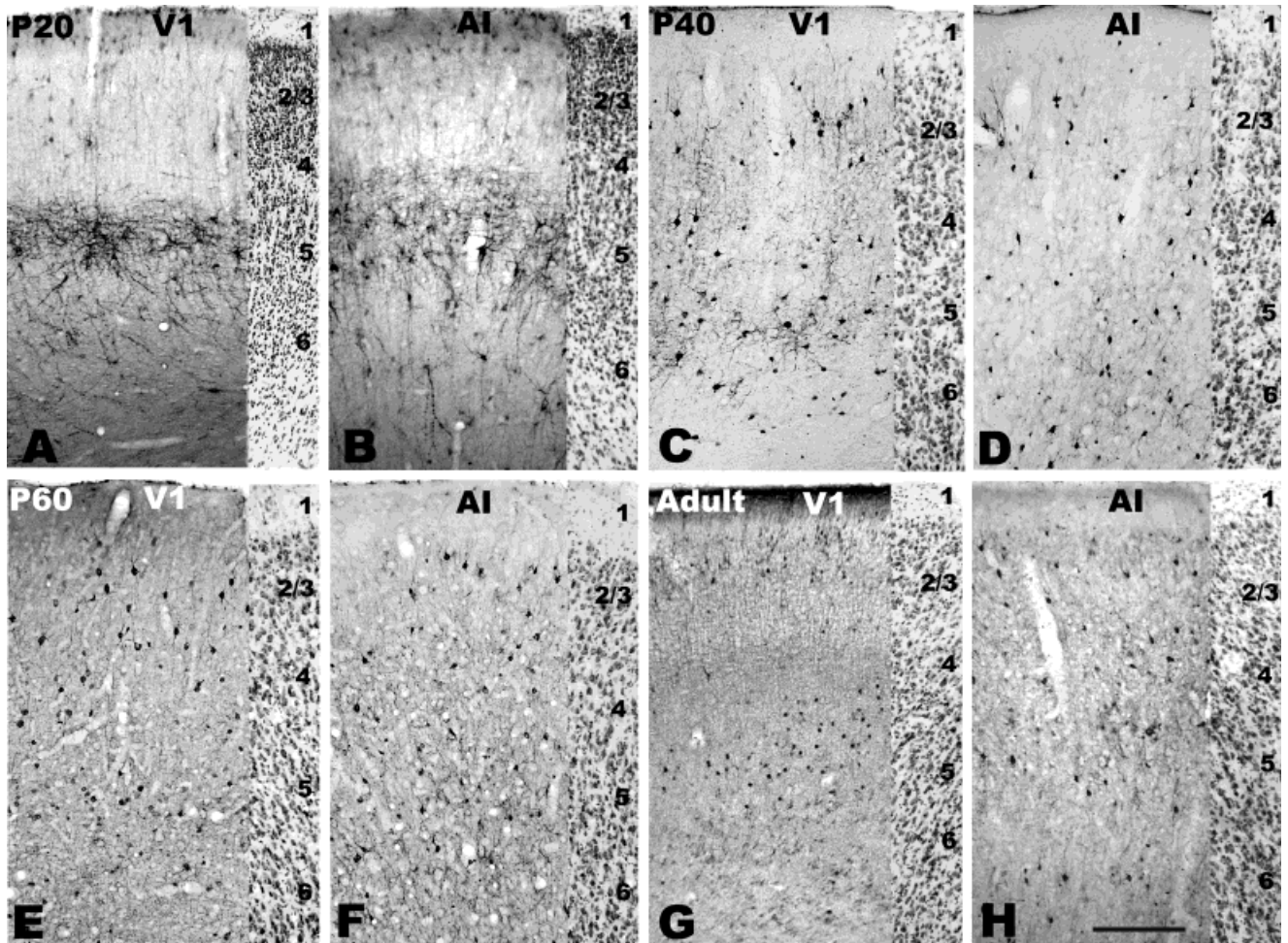


Fig. 4. Late postnatal development of PV-ir neurons in V1 (A,C,E,G) and AI (B,D,F,H) from P20 to adulthood. At P20 (A,B), the density of PV-ir neurons was low, and parvalbumin was expressed mainly in the dendrites and axons of the neurons in layer 5 and 6, and in the white matter. Some neurons located in layer 1 and the superficial part of 2/3 also weakly and transiently expressed parvalbumin.

By P40 (C,D), there were PV-ir neurons distributed throughout the cortical layers except layer I. PV-ir neurons were fewer in number in layer 4 of V1 but were more evenly distributed in all layers from layer 2/3 to 6 of AI. Moreover, both the distribution and number were similar to those at P60 (E,F) and adulthood (G,H). Scale bar = 200  $\mu$ m.

and axons with their axonal varicosities, of deep layer nonpyramidal neurons began to express CB strongly (Fig. 9G,H), allowing a glimpse of their early morphology. At P20 and older ages, the morphology of these CB-ir neurons progressively matured (Fig. 10). The nonpyramidal CB-ir neurons exhibited markedly different morphologies than the nonpyramidal PV-ir neurons from P20 onward (compare Figs. 4 and 8 with Figs. 6 and 10). The CB-ir neurons had small to medium-sized somata and mainly a bipolar or double bouquet morphology (cf. Fairén et al., 1984), whereas some of the PV-ir neurons had much larger somata and a multipolar morphology. After P20, these morphological differences between PV-ir and CB-ir neurons became more apparent (Figs. 8, 10).

### Comparison of cell size

Soma sizes were measured in the context of the Abercrombie correction procedure and are presented in Table 2. As expected, the soma areas of Nissl-stained neurons

were generally smaller at early than at late ages. Neurons in AI were larger on average than those in V1, and this difference was significant at all ages except P7 and P14. Apart from this observation, however, there were no consistent trends. The soma size comparison for the CB-ir neurons showed that AI neurons were larger than V1 neurons at early but not at later stages. PV-ir neurons were largely similar in size between AI and V1 in the stages prior to P14, but their size relationship became variable in later stages. We also observed that, at P1 and P7, the PV- and CB-ir neurons had larger somata than the Nissl-stained total neuronal population. However, this was no longer true at later stages, perhaps due to the loss of the transient staining in the pyramidal cell population. The soma size distributions did not differ in any consistent way between PV- and CB-ir neurons at each postnatal age, probably due to the multiple cell types composing each group, each with different soma sizes, which might have been changing in size with different time courses

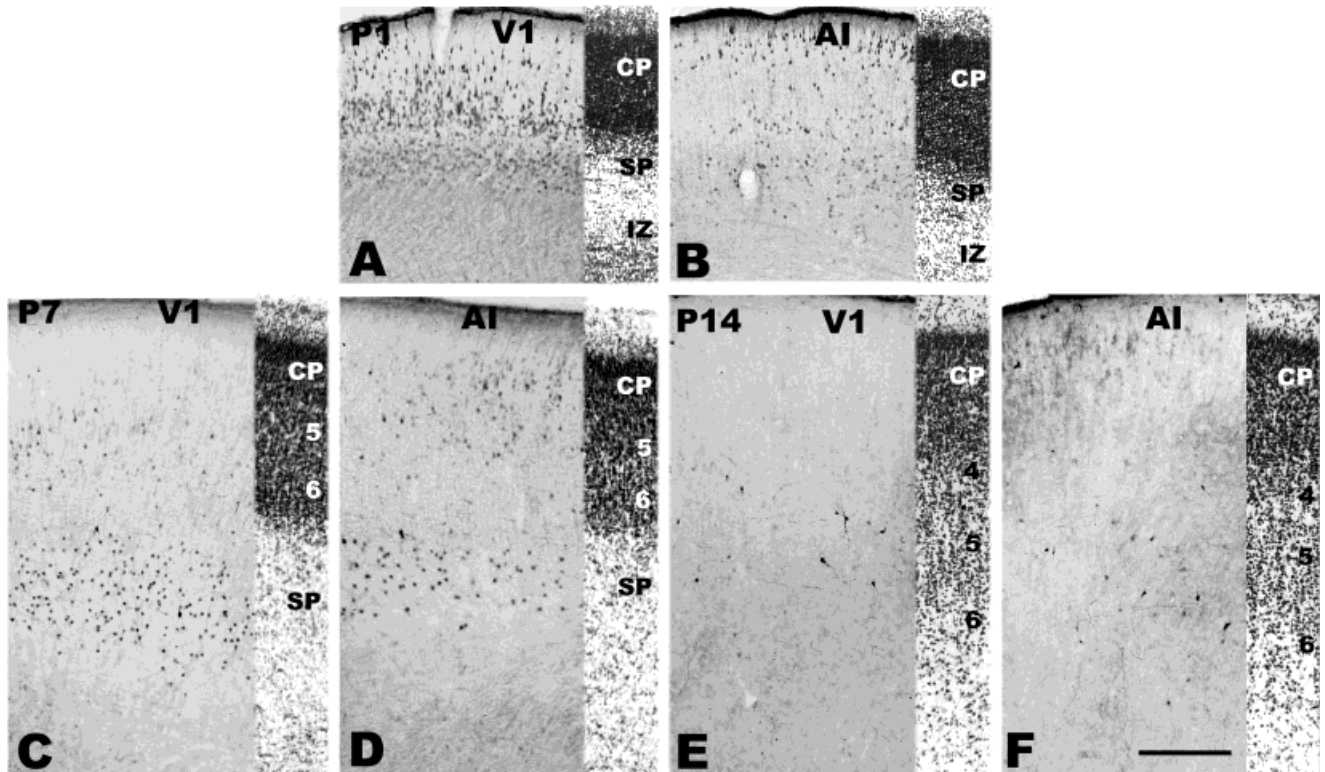


Fig. 5. Early postnatal development of CB-ir neurons in ferret V1 (A,C,E) and AI (B,D,F). At P1 (A,B), CB-ir neurons were distributed in both the cortical plate (CP) and subplate (SP), with few neurons in the marginal zone. No immunoreactive neurons were seen in the intermediate zone (IZ). By P7 (C,D), the labeled neurons in layer 1 disappeared,

but the neurons in the subplate still expressed calbindin strongly. At P14 (E,F), the number of calbindin-ir neurons decreased dramatically to a very low level. As observed with parvalbumin expression, very few neurons in layers 5 and 6 contained detectable levels of calbindin. Scale bar = 200  $\mu$ m.

over development. In particular, the PV- and CB-ir pyramidal neurons had large somata, and the loss of the transient staining in this subgroup would affect the mean soma size substantially. In this study we did not attempt to differentiate between subtypes of PV-ir or CB-ir neurons for quantitative purposes. Such a comparison would require a labeling technique that revealed the dendritic and axonal arbors more completely and to the same extent at each age in each group. It was apparent that the CB antibody generally revealed more of the arborizations than did the PV antibody.

#### Density of PV- and CB-ir neurons

Somata in Nissl-stained 50- $\mu$ m sections and CB-ir or PV-ir somata in adjacent 30- $\mu$ m sections were counted to arrive at quantitative estimates of neuron number per cortical column (density). [Nissl data were taken from Gao et al. (1999).] The Abercrombie method was used for split cell corrections (Abercrombie, 1946; Guillery and Herrup, 1997). Somata and not nucleoli were used for counts because nucleoli were obscured in the immunostained material. Density estimates were calculated by dividing the number of somata counted by the area of cortex in which they resided. Area and not volume measures were used because of the incomplete penetrance of the antibody in 30- $\mu$ m or thicker sections. The values presented here should be interpreted as estimates, not absolute values, due to the choice of counting method (Popken and Farel,

1996; Guillery and Herrup, 1997). Figure 11 shows the results of counts of PV-ir and CB-ir neurons throughout cortical development. As reported previously (Gao et al., 1999), density of all neurons is high in the cortical plate at P1, and this was also true of the PV- and CB-containing neurons. Thereafter, neuronal density sharply declined during the period of programmed cell death and expansion of the cortical lobes. The decline in neuronal density was very sharp from P7 to P20; thereafter density differed little (PV-ir, Fig. 11A; CB-ir, Fig. 11B) until adulthood. Note that P20 in ferrets is approximately equivalent to P1 in cats (Luskin and Shatz, 1985a; Jackson et al., 1989; Ruthazer et al., 1999). There were no consistent differences between V1 and AI observed in these density measurements.

#### Proportion of PV-ir and CB-ir neurons

Proportional changes in immunoreactive neurons relative to Nissl-stained neurons are obscured by the wholesale decrease in total numbers of neurons over development. Measurement of the proportions of the immunoreactive neurons was thus performed to reveal interesting relationships between populations. The proportions (percent of total Nissl-stained neurons) of both PV- and CB-ir neurons peaked at P1 and then sharply declined to P20, where they reached their lowest point (0.7–1.2%) during the entire postnatal developmental process (Fig. 12A,B). This was true in both V1 and AI. Fol-

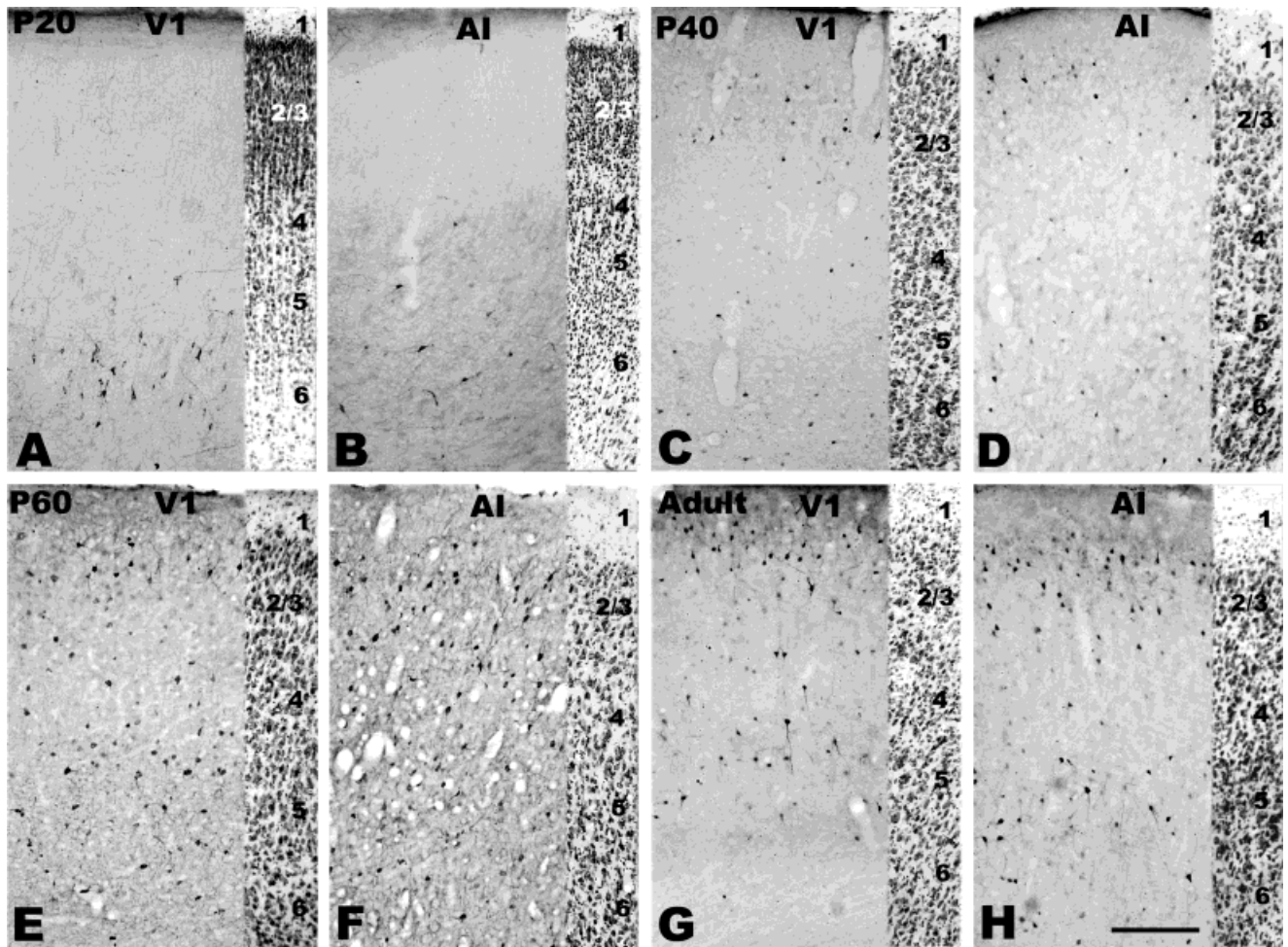


Fig. 6. Late postnatal development of CB-ir neurons in V1 (A,C,E,G) and AI (B,D,F,H) from P20 to adulthood. At P20 (A,B), calbindin-immunopositive neurons could be observed mainly in layer 5 and 6, but particularly in layer 6. The number of CB-ir somata decreased to its lowest postnatal level at P20, but axonal labeling could be observed. By P40 (C,D), the CB-ir pattern was bilaminar, with a dense band of calbindin-ir cells in layer 2/3 and a second band

in layers 5 and 6. There were almost no CB-ir neurons in layers 1 or 4. The bilaminar P40 pattern was similar to the distribution pattern of CB-ir neurons in adulthood (G,H), but at P60 (E,F) the CB-ir neurons were widespread throughout layers 2–6, due to a transient increase in CB immunoreactivity in the middle layers. Scale bar = 200  $\mu$ m.

lowing P20, PV-ir neurons exhibited a steady increase in their proportion from P20 to P40. From this point, some differences were seen between V1 and AI neurons and between PV-ir and CB-ir neurons. The proportion of PV-ir neurons increased from P60 to adulthood in V1 and AI. In contrast, the proportion of CB-ir neurons decreased slightly from P60 to adulthood in both V1 and AI. These results suggested that the PV-ir neuronal composition was not mature until adulthood, whereas the CB-ir neurons were relatively mature in their final proportion at approximately P60.

## DISCUSSION

Parvalbumin and calbindin D-28K are calcium-binding proteins expressed in two non-overlapping subpopulations of GABA-ir interneurons in adult primate neocortex (Hendry et al., 1989), as well as that of cats (Hendry and Jones, 1991; Hogan et al., 1992; Hogan and Berman, 1993), a

carnivore closely related to ferrets, and rodents (Del Río et al., 1994; Gonchar and Burkhalter, 1997). The developmental distribution of calcium-binding proteins in cerebral cortex has been described in several mammalian species (Stichel et al., 1987; Hendrickson et al., 1991; Hogan et al., 1992; Alcántara et al., 1993, 1996a; Hogan and Berman, 1993, 1994; Del Río et al., 1994; Friauf, 1994; Conde et al., 1996; Yan et al., 1997; Letinic and Kostovic, 1998) but not in an altricial carnivore such as the ferret. Ferrets are particularly valuable for research on cortical development because of their short gestation period and the relative immaturity of their cortex at birth compared with other mammals. Although the overall time course and length of ferret brain development is similar to that in cats, a closely related carnivore, ferrets are born much earlier in the cortical developmental process, at the point where only layers 5 and 6 of cortex have formed, 2–3 weeks prior to the ingrowth of thalamocortical axons (Luskin and Shatz, 1985a; Jackson et al., 1989), and 4

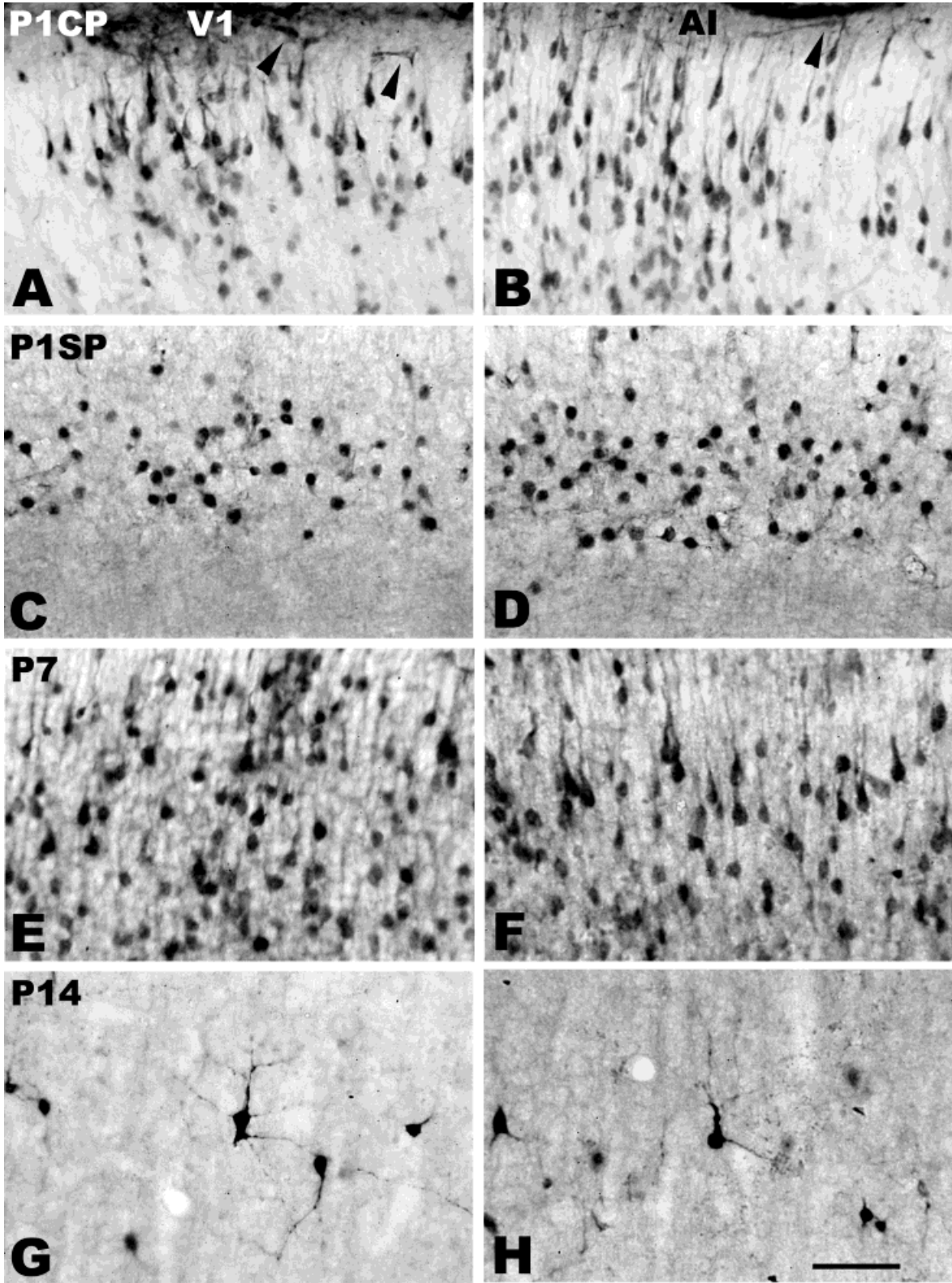


Fig. 7. Higher magnification photomicrographs at early stages of postnatal development, showing the morphological development of PV-ir neurons in V1 (A,C,E,G) and AI (B,D,F,H). At P1 (A,B), several horizontally oriented PV-ir neurons (arrowheads) were seen in the marginal zone (MZ) of the cortical plate (CP) and were presumably Cajal-Retzius neurons. This transient population of neurons no longer expressed PV by P7. Most of the PV-ir neurons in the cortical plate at

P1 and P7 (E,F) were pyramidal in shape. In contrast, the PV-ir neurons distributed in the subplate (SP) (C,D) were small, spherical, and tadpole-shaped. By P14, PV immunoreactivity decreased to low levels, and very few neurons in layers 5 and 6 expressed it. The morphologies of the PV-ir neurons were complex and generally similar to those at later stages, but they were smaller in size. Scale bar = 50  $\mu$ m.

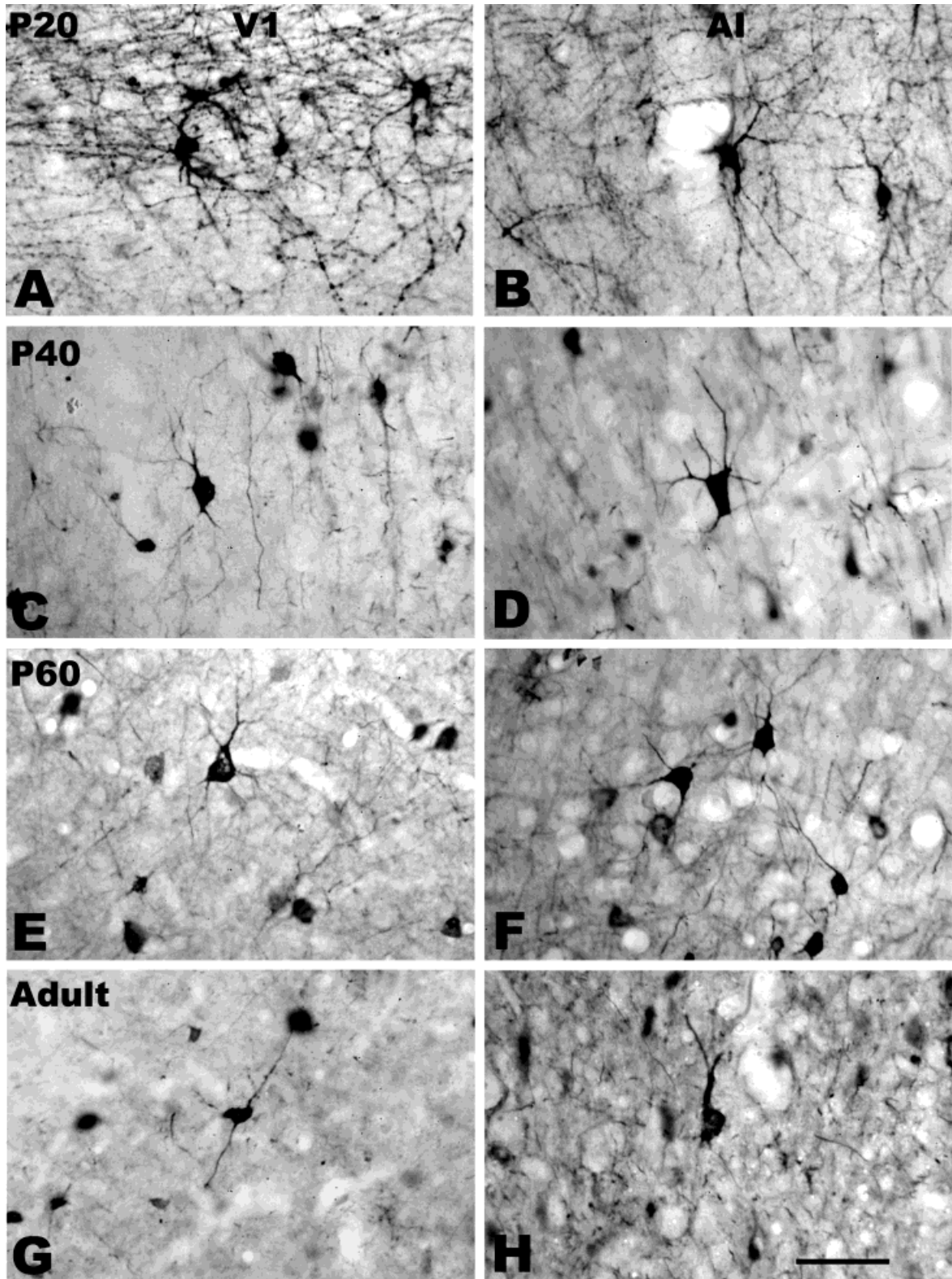


Fig. 8. Photomicrographs illustrating the morphology of PV-ir neurons at later postnatal stages. At P20 (**A,B**), the neurons in layer 5 strongly expressed parvalbumin, especially in their dendrites and axons, which formed a network-like arrangement in both the deep cortical layers and the white matter. Note the varicosities on the

processes. At P40 (**C,D**), PV immunoreactivity decreased in the dendrites and axons but increased in the somata. However, at P40 both the morphology and the size of the PV-ir neurons were generally similar to that seen at P60 (**E,F**) and adulthood (**G,H**). Scale bar = 50  $\mu$ m.

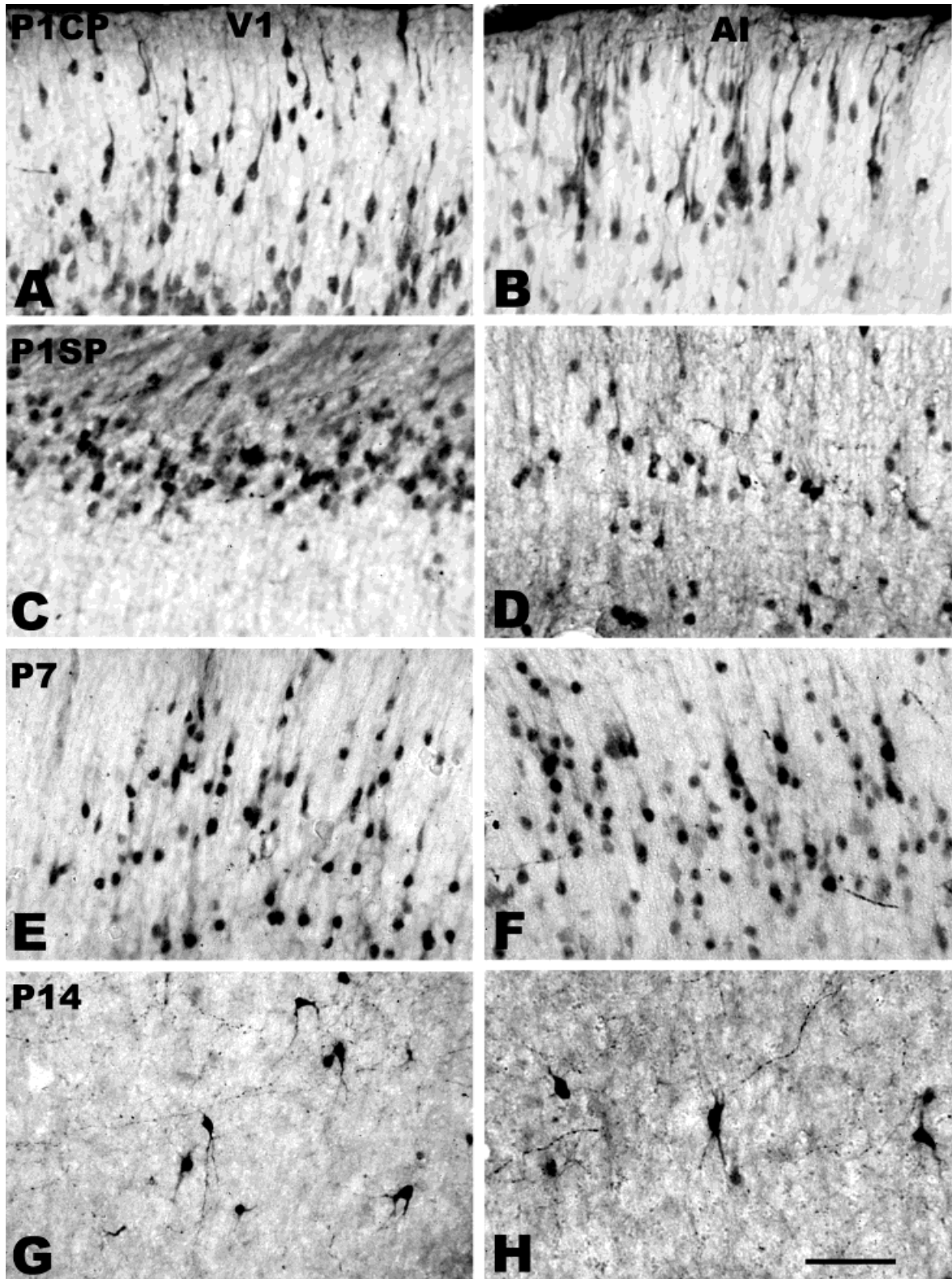


Fig. 9. High-magnification photomicrographs showing the morphology of CB-ir neurons in early postnatal development in V1 (A,C,E,G) and AI (B,D,F,H). At P1 (A–D), the CB-ir neurons could be observed in the marginal zone (A). The immunopositive neurons in the cortical plate (CP) were bipolar or pyramidal in morphology in both V1 and AI. In the subplate (SP), the CB-ir neurons were spher-

ical and tadpole-shaped (C). By P7, the CB-ir neurons in the MZ disappeared, and calbindin began to appear in axonal and dendritic processes. By P14, pyramidal neurons no longer expressed calbindin, and most of the immunopositive neurons in layers 5 and 6 had a double bouquet or bipolar morphology, as apparent from the strong dendritic labeling. Scale bar = 50  $\mu$ m.

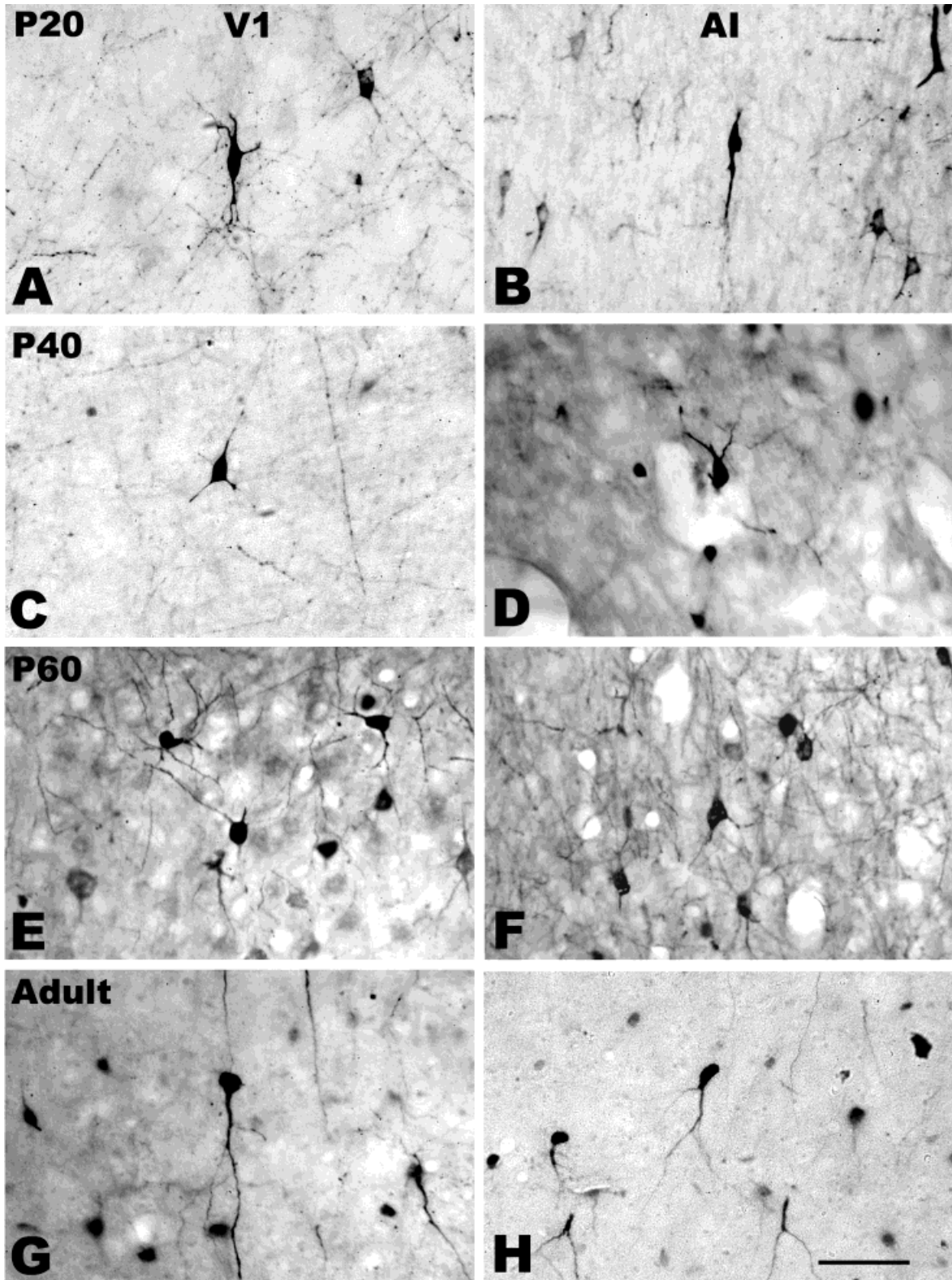


Fig. 10. Late morphological development of CB-ir neurons from P20 to adulthood. At P20 (**A,B**), calbindin was strongly expressed in both dendrites and axons. As seen earlier in development, the CB-ir neurons at P20 and later stages had a bipolar or double bouquet morphology. At P40 and afterward (**C-F**), the morphology resembled

that seen in the adult (**G,H**) and was strikingly different from the morphology of PV-ir neurons (Fig. 8). There were no apparent morphological differences in CB-ir neurons between V1 and AI. Scale bar = 50  $\mu$ m.

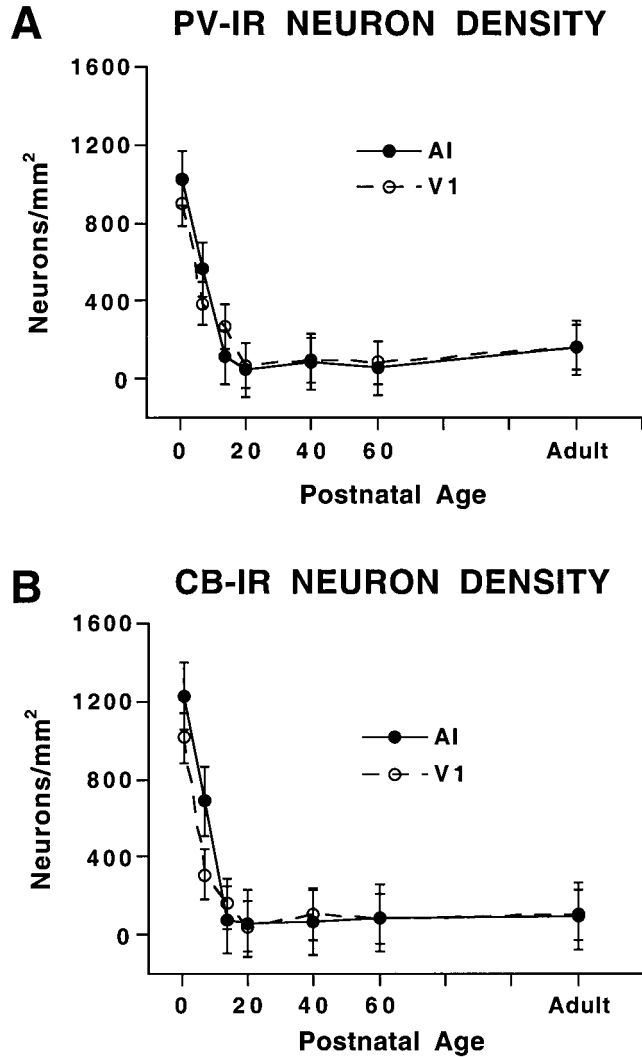


Fig. 11. Developmental changes in PV- and CB-ir neuron density. **A:** Quantitation of PV-ir neuron density during postnatal development. PV-ir neuron density was highest at P1 in both V1 and AI and declined dramatically to its lowest level at P20. Thereafter, it remained fairly constant until adulthood. **B:** Quantitation of CB-ir neuron density during postnatal development. Neuronal density was highest at P1 and declined to its lowest level at P20. Thereafter, it was relatively stable until adulthood. The time course of changes in density of PV- and CB-ir neurons was similar in V1 and AI.

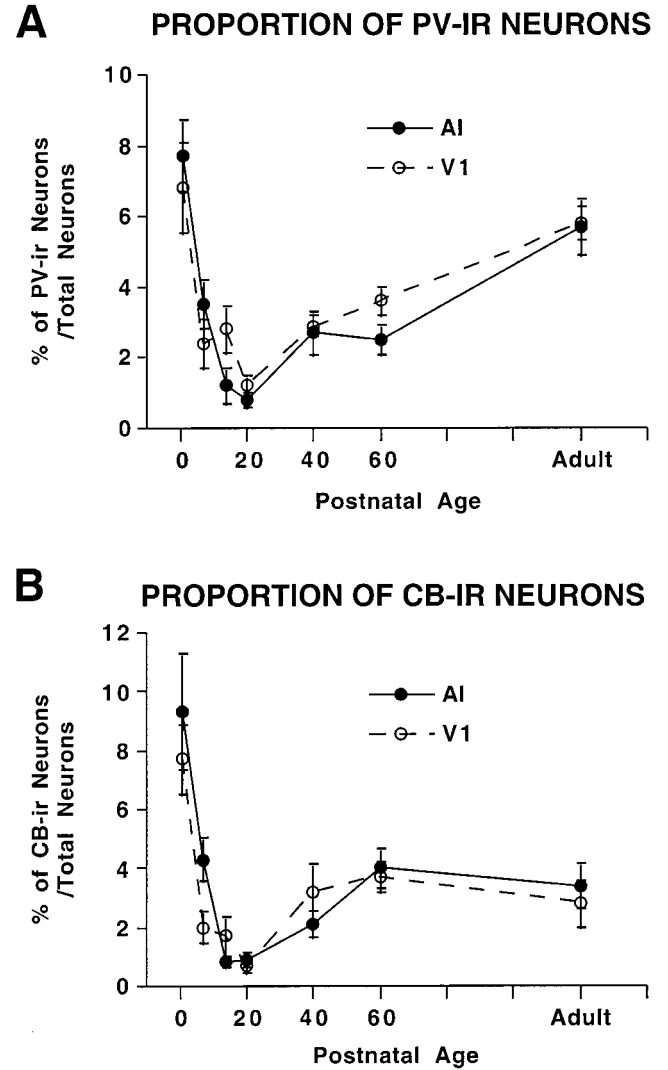


Fig. 12. The proportion of both PV- and CB-ir neurons was also quantified by calculating the number of immunoreactive neurons as a percent of Nissl-stained (total) neurons, given that total neuronal density declines sharply during postnatal development. The proportion of PV-ir neurons (**A**) and CB-ir neurons (**B**) was at a maximum at P1 and a minimum at P20. Thereafter, the proportion of PV-ir neurons increased gradually until adulthood, whereas the CB-ir neurons exhibited a secondary peak at P60, with a slight decrease in adulthood. There were no consistent differences between the two cortical areas.

weeks prior to eye (Cucchiario and Guillery, 1984) and ear canal (Moore and Hine, 1992) opening. By employing ferrets, this study has provided more detailed data for understanding the early development of chemoarchitecture in mammalian sensory cortex.

We find that PV and CB are expressed at their highest postnatal levels at birth, in both pyramidal and nonpyramidal neurons, after which expression declines precipitously, up to the stage that is equivalent to P1 in cats. Later in postnatal development, near the close of the critical period for ocular dominance plasticity (Issa et al., 1999; Ruthazer et al., 1999), PV and CB expression in nonpyramidal neurons increases, suggesting involvement

of these calcium-binding protein-containing neurons in late, experience-dependent stages of cortical development.

### Comparison between V1 and AI

Although numerous studies have been done in visual cortical areas, there are only a small number of studies addressing the distribution of calcium-binding proteins in mammalian auditory cortical neurons (e.g., Hendry and Jones, 1991; McMullen et al., 1994), and none of these from a developmental perspective. Hendry and Jones (1991) found in adult cat AI that PV- and CB-ir neurons represented completely non-overlapping subpopulations of GABA-containing nonpyramidal neurons. No pyramidal

neurons were found to contain GABA, PV, or CB. PV-ir neurons had the morphology of basket and chandelier cells, and CB-ir neurons resembled double bouquet neurons, as seen in primate and cat visual cortex (Hendry et al., 1989; Alcántara and Ferrer, 1994, 1995).

In the present study, only minor differences were seen in either the qualitative or quantitative pattern of PV and CB expression between V1 and AI in developing ferret sensory neocortex. The developmental changes in density and proportion of PV-ir and CB-ir neurons were similar in both cortical areas, although the auditory cortex develops in general somewhat earlier than does V1, given its more rostral position. A related study (Alcántara and Ferrer, 1995) also reported no obvious maturational gradient in calbindin staining. In addition, the laminar development of immunostaining occurred approximately in parallel for V1 and AI. The absence of striking differences between areas V1 and AI in pattern and time course of maturation of expression of these two calcium-binding proteins suggests coordinated development of cortical inhibitory circuits among cytoarchitectonically and functionally distinct cortical areas.

#### Distribution pattern of PV- and CB-ir neurons in V1 and AI during development

In a previous study of the postnatal development of GABA-ir neurons (Gao et al., 1999), we reported that the proportion of GABA-ir neurons in primary visual and primary auditory cortex peaked early (at P1), when most of the neurons have yet to migrate in to the cortical plate. It then declined by P20, when most of the neurons were in their final location, peaked secondarily later in cortical development (at P60), and then declined again by adulthood. The secondary peak was higher (~15% of total neurons) than the first (~8% of total neurons). In the present study, one goal was to determine whether a particular subclass of GABA-ir neurons was responsible for the early and late peaks. We found that the proportions of both PV-ir and CB-ir neurons had an early postnatal peak at P1, followed by a decline by P20 and then a second peak late in development; however, the early peak is substantially larger than the later peak for both cell types. Neither the individual late peaks in PV- (~3% of total neurons) and CB-ir cells (~4% of total neurons) nor the combined total (~7% of total neurons) were of sufficient magnitude to explain the secondary peak in GABA-ir neurons entirely, suggesting that another subpopulation of GABA-ir neurons must contribute to the total GABA-ir population, perhaps calretinin-containing neurons (Fonseca et al., 1995; Yan et al., 1995a). Also, although the combined proportion of PV-ir and CB-ir neurons estimated in this study accounts for only about half the proportion of GABA-ir neurons at P60 (Gao et al., 1999), they compose approximately three-quarters in adulthood, suggesting that there may be another subpopulation of GABA-ir neurons that declines markedly between P60 and adulthood. Double-labeling studies are in progress to address these issues.

The laminar pattern of PV- and CB-immunoreactivity in P20 and older ferrets is similar to that obtained from postnatal cat primary visual or somatosensory cortex (Stichel et al., 1987; Alcántara and Ferrer, 1994, 1995; Hogan and Berman, 1994), where it was reported that PV follows the inside-out gradient of laminar development in neocortex, and that CB is found in infragranular layers in

early postnatal development, and in infragranular and supragranular layers at maturity. However, it must be taken into account that these postnatal cat studies began their analyses at the equivalent of P21 in ferrets. At birth in ferrets we observed heavy immunolabeling for both PV and CB in the cortical plate, subplate, and developing infragranular layers. From P14 to P20, the immunolabeling declined precipitously in all layers. P40 lamination patterns resembled the adult pattern, but at P60, the bilaminar pattern of CB-immunoreactivity was transiently lost, only to be regained in adulthood. This has not been reported in other species. With the methods used in this study, we cannot determine whether the transient widespread distribution of neurons expressing CB at P60 results from addition of new CB-ir neurons, from a sudden acquisition and then loss of CB immunoreactivity in a subpopulation of neurons, or from an increase in the detectable levels of CB. However, it seems highly unlikely that new neurons would be added in the middle layers of cortex at this late stage of cortical development (Luskin and Shatz, 1985a; Jackson et al., 1989). Because CB is a calcium-binding protein that functions to sequester calcium in neurons that are metabolically active (see McBurney and Neering, 1987, for review), the data suggest that this subpopulation of neurons plays an especially active role in late stages of cortical development. Further studies are needed to determine their functional role.

#### Morphological development of immunoreactive neurons

We observed both pyramidal and nonpyramidal neurons containing PV or CB in this study. Pyramidal neurons expressing calcium-binding proteins in adult cerebral cortex have been reported in several mammals (Hof et al., 1999), including sensory cortex in macaques (Kondo et al., 1994; Preuss and Kaas, 1996), cats (Stichel et al., 1987), rabbits (De Venecia et al., 1998), and rats (van Brederode et al., 1991). In contrast, a study of adult cat auditory cortex found that all PV- or CB-containing neurons were nonpyramidal and also contained GABA (Hendry and Jones, 1991). The differences seen may be actual species differences and/or differences between cortical areas. Alternatively, they may be due to variations in techniques or antibodies used or even in how pyramidal neurons are defined morphologically.

In ferrets we found large numbers of PV-ir and CB-ir pyramidal neurons in the cortical plate prior to P14 but did not see such neurons after this age. Pyramidal neurons containing PV or CB are found in striate cortex of prenatal monkeys (Hendrickson et al., 1991), neonatal cats (Hogan and Berman, 1993, 1994; Alcántara and Ferrer, 1994, 1995), neonatal mouse (Del Río et al., 1992), and neonatal rat (Alcántara et al., 1993). There appears to be a species difference in the overall temporal expression pattern of PV- and CB-ir pyramidal neurons in cats and ferrets, since in cats they are not lost until after P21, which corresponds to 4 weeks after their disappearance in ferrets. It would thus be interesting to explore the role of spontaneous activity in the regulation of calcium-binding protein expression.

PV- and CB-ir neurons in ferret V1 and AI shared a similar morphology during early postnatal development, appearing in pyramidal and tadpole-shaped neurons located in the cortical plate and subplate, respectively. However, starting from P20, the PV-ir and CB-ir neurons

began to differentiate morphologically. At this point, most of the PV-ir neurons were multipolar, with the morphology of large basket and chandelier neurons. In contrast, the majority of the CB-ir neurons were spindle-shaped bipolar or double bouquet cells with dendrites emanating vertically from either side of the soma. The markedly different morphology of CB-ir compared with PV-ir neurons supports evidence from other species that they represent different functional cell types in adults and that this is true during development as well (Demeulemeester et al., 1989; Hendry et al., 1989; Celio, 1990; Alcántara and Ferrer, 1994, 1995; Hogan and Berman, 1994).

We found a number of horizontally oriented PV-ir neurons with thick dendrites in layer 1 early in development but not at later stages. Occasionally, similar neurons were observed to label with the CB antibody. We propose that these are Cajal-Retzius cells. Previous studies in monkeys have demonstrated the simultaneous presence of multiple calcium-binding proteins in Cajal-Retzius cells (Huntley and Jones, 1990; Yan et al., 1995b). These cells typically disappear or become hard to detect in adult cortex (Luskin and Shatz, 1985b; Marin-Padilla, 1988, 1998). In a previous study, we found cells of this morphological type that contained GABA (Gao et al., 1999), and they may represent the same cell type.

The combined PV-ir and CB-ir populations accounted for approximately 16% of the total neurons at P1, whereas GABA-ir neurons formed only approximately 8% of the total, raising the possibility that at these very early stages of development, calcium-binding proteins are transiently found in non-GABA-ir neurons. Pyramidal neurons are generally thought not to express GABA, although in a previous study we observed GABA-ir pyramidal neurons in V1 and AI (Gao et al., 1999). It is possible that some proportion of the population of PV- and/or CB-ir pyramidal neurons also contains GABA, and this could be addressed with a double-labeling study. The functional significance of the transient GABA and calcium-binding protein expression in pyramidal neurons remains speculative. We propose that PV and CB may be important in excitatory synaptic transmission and/or neurotrophic support at these early stages, or that they function in calcium regulation in a temporary capacity.

### Significance for understanding cortical developmental mechanisms

The complex time course of changes in calcium-binding protein expression in ferret sensory neocortex suggests that they or the neurons in which they reside play different roles at different stages of development. The time of appearance of these calcium-binding proteins in relation to developmental events can be used to constrain their possible functional roles.

Some previous studies in cats have shown that neurons immunoreactive for calcium-binding proteins such as PV and CB appear in large numbers only late in cortical development, and one suggestion has been that the expression of calcium-binding proteins is triggered by thalamocortical pathway formation (Stichel et al., 1987; Hendrickson et al., 1991; Alcántara and Ferrer, 1994, 1995; Blümcke et al., 1994; Hogan and Berman, 1994; Alcántara et al., 1996b; Carder et al., 1996; Vogt Weisenhorn et al., 1998). The appearance of CB correlated with the onset of the thalamocortical projections in some cases (Hendrickson et al., 1991; Hogan and Berman, 1994;

Letinic and Kostovic, 1998). In monkeys and rats, PV does not appear until after birth and correlates with the time of eye opening, not thalamocortical innervation (Hendrickson et al., 1991; Alcántara et al., 1993). However, in ferret primary sensory neocortex, we found that both PV- and CB-ir neurons appeared at least by the first postnatal day. This early appearance preceded thalamocortical innervation but coincided temporally with the migration and functional maturation of cortical neurons. Thalamocortical innervation in ferrets is under way at P20, and cortical neuronal migration is complete at about P30 (Jackson et al., 1989; Chapman and Stryker, 1993). At this point, the density and proportion of PV and CB had also dropped to their lowest level. Therefore, calcium-binding proteins might be involved in neuronal migration and maturation in early cortical development, but their initial expression is probably not triggered by thalamocortical activity.

The precipitous drop in PV- and CB-immunoreactivity between P7 and P20 may simply result from a loss of expression in pyramidal neurons, followed by a delay in increased expression in nonpyramidal neurons. Another interesting though not mutually exclusive possibility is that the change in calcium-binding protein expression reflects a change in the function of GABA-ir neurons during development. In neonatal rats, GABA is released nonsynaptically and may play a trophic role (Gordon-Weeks et al., 1984; Lauder, 1993). Early in postnatal neocortical development, GABA produces depolarizing potentials in postsynaptic neurons that can activate voltage-gated calcium channels (Yuste and Katz, 1991; LoTurco et al., 1995; Owens et al., 1996). After this early stage, GABA gradually becomes inhibitory to postsynaptic neurons (Cherubini et al., 1991; Hensch et al., 1998). We suggest that the biphasic pattern of calcium-binding protein expression results from the switch in GABA function from excitatory to inhibitory. Calcium-binding proteins would be especially important for regulation of calcium levels during the period when GABA as well as glutamate (through N-methyl-D-aspartate receptors) can trigger calcium influx into postsynaptic neurons, but they might be less important when GABA opens chloride channels. We propose that the reappearance of elevated calcium-binding protein levels at P60 or later is related to experience-dependent fine-tuning of cortical circuitry late in the critical period. Recent physiological and molecular studies showing the importance of inhibitory circuitry in activity-dependent refinement of central sensory circuits during development (Hensch et al., 1998; Zheng and Knudsen, 1999) are consistent with this idea.

### ACKNOWLEDGMENTS

We thank Joseph Nelson, Shaun Daugherty, Jennifer Power, and Pat Ramachandran for technical assistance, Drs. Kathrin Herrmann, Max Cynader, and Qiang Gu for valuable discussions, and Drs. Vincent Rehder and Paul Katz for their comments on the manuscript. S.L.P. received grants from the Georgia Research Alliance, NSF, and the Whitehall Foundation, and A.W. received an NIH Summer Medical and Research Training grant through Baylor College of Medicine.

## LITERATURE CITED

- Abercrombie M. 1946. Estimation of nuclear populations from microtome sections. *Anat Rec* 94:239–247.
- Alcántara S, Ferrer I. 1994. Postnatal development of parvalbumin immunoreactivity in the cerebral cortex of the cat. *J Comp Neurol* 348:133–149.
- Alcántara S, Ferrer I. 1995. Postnatal development of calbindin-D28k immunoreactivity in the cerebral cortex of the cat. *Anat Embryol (Berl)* 192:369–384.
- Alcántara S, Ferrer I, Soriano E. 1993. Postnatal development of parvalbumin and calbindin D28K immunoreactivities in the cerebral cortex of the rat. *Anat Embryol (Berl)* 188:63–73.
- Alcántara S, De Lecea L, Del Río JA, Ferrer I, Soriano E. 1996a. Transient colocalization of parvalbumin and calbindin D28k in the postnatal cerebral cortex: evidence for a phenotypic shift in developing nonpyramidal neurons. *Eur J Neurosci* 8:1329–1339.
- Alcántara S, Soriano E, Ferrer I. 1996b. Thalamic and basal forebrain afferents modulate the development of parvalbumin and calbindin D28k immunoreactivity in the barrel cortex of the rat. *Eur J Neurosci* 8:1522–1534.
- Allison JD, Kabara JF, Snider RK, Casagrande VA, Bonds AB. 1996. GABA<sub>B</sub>-receptor-mediated inhibition reduces the orientation selectivity of the sustained response of striate cortical neurons in cats. *Vis Neurosci* 13:559–566.
- Antonopoulos J, Pappas IS, Parnavelas JG. 1997. Activation of the GABA<sub>A</sub> receptor inhibits the proliferative effects of bFGF in cortical progenitor cells. *Eur J Neurosci* 9:291–298.
- Behar TN, Li YX, Tran HT, Ma W, Dunlap V, Scott C, Barker JL. 1996. GABA stimulates chemotaxis and chemokinesis of embryonic cortical neurons via calcium-dependent mechanisms. *J Neurosci* 16:1808–1818.
- Berman AL, Jones EG. 1982. The thalamus and basal telencephalon of the cat. Madison: University of Wisconsin Press.
- Berman NJ, Douglas RJ, Martin KAC. 1992. GABA-mediated inhibition in the neural networks of visual cortex. In: Mize RR, Marc RE, Sillito AM, editors. *Progress in brain research*, vol 90. New York: Elsevier. p 443–476.
- Berninger B, Marty S, Zafra F, Da Penha Berzaghi M, Thoenen H, Lindholm D. 1995. GABAergic stimulation switches from enhancing to repressing BDNF expression in rat hippocampal neurons during maturation in vitro. *Development* 121:2327–2335.
- Blümcke I, Weruaga E, Kasas S, Hendrickson AE, Celio MR. 1994. Discrete reduction patterns of parvalbumin and calbindin D-28k immunoreactivity in the dorsal lateral geniculate nucleus and the striate cortex of adult macaque monkeys after monocular enucleation. *Vis Neurosci* 11:1–11.
- Carder RK, Leclerc SS, Hendry SHC. 1996. Regulation of calcium-binding protein immunoreactivity in GABA neurons of macaque primary visual cortex. *Cereb Cortex* 6:271–287.
- Cauli B, Audinat E, Lambolez B, Angulo MC, Ropert N, Tsuzuki K, Hestrin S, Rossier J. 1997. Molecular and physiological diversity of cortical nonpyramidal cells. *J Neurosci* 17:3894–3906.
- Celio MR. 1990. Calbindin D-28k and parvalbumin in the rat nervous system. *Neuroscience* 35:375–475.
- Celio MR, Baier W, Schärer L, De Viragh PA, Gerday C. 1988. Monoclonal antibodies directed against the calcium binding protein parvalbumin. *Cell Calcium* 9:81–86.
- Celio MR, Baier W, Schärer L, Gregersen HJ, De Viragh PA, Norman AW. 1990. Monoclonal antibodies directed against the calcium binding protein calbindin D-28k. *Cell Calcium* 11:599–602.
- Chapman B, Stryker MP. 1993. Development of orientation selectivity in ferret visual cortex and effects of deprivation. *J Neurosci* 13:5251–5262.
- Chapman B, Zahs KR, Harris SL, Stryker MP. 1996. Plasticity following monocular deprivation in ferret primary visual cortex. *Soc Neurosci Abstr* 22:1727.
- Cherubini E, Gaiarsa JL, Ben-Ari Y. 1991. GABA: an excitatory transmitter in early postnatal life. *Trends Neurosci* 14:515–519.
- Conde F, Lund JS, Lewis DA. 1996. The hierarchical development of monkey visual cortical regions as revealed by the maturation of parvalbumin-immunoreactive neurons. *Brain Res Dev Brain Res* 96:261–76.
- Crook JM, Eysel UT. 1992. GABA-induced inactivation of functionally characterized sites in cat visual cortex (area 18): effects on orientation tuning. *J Neurosci* 12:1816–1825.
- Crook JM, Kisvárdy ZF, Eysel UT. 1998. Evidence for a contribution of lateral inhibition to orientation tuning and direction selectivity in cat visual cortex: reversible inactivation of functionally characterized sites combined with neuroanatomical tracing techniques. *Eur J Neurosci* 10:2056–2075.
- Crook JM, Kisvárdy ZF, Eysel UT. 1996. GABA-induced inactivation of functionally characterized sites in cat visual cortex (area 18): effects on direction selectivity. *J Neurophysiol* 75:2071–2088.
- Crook JM, Kisvárdy ZF, Eysel UT. 1997. GABA-induced inactivation of functionally characterized sites in cat striate cortex: effects on orientation tuning and direction selectivity. *Vis Neurosci* 14:141–158.
- Cucchiari J, Guillery RW. 1984. The development of the retinogeniculate pathways in normal and albino ferrets. *Proc R Soc Lond B* 223:141–164.
- Das A, Gilbert CD. 1999. Topography of contextual modulations mediated by short-range interactions in primary visual cortex. *Nature* 399:655–661.
- De Venecia RK, Smelser CB, McMullen NT. 1998. Parvalbumin is expressed in a reciprocal circuit linking the medial geniculate body and auditory neocortex in the rabbit. *J Comp Neurol* 400:349–362.
- Del Río JA, Soriano E, Ferrer I. 1992. Development of GABA-immunoreactivity in the neocortex of the mouse. *J Comp Neurol* 326:501–526.
- Del Río JA, De Lecea L, Ferrer I, Soriano E. 1994. The development of parvalbumin-immunoreactivity in the neocortex of the mouse. *Brain Res Dev Brain Res* 81:247–259.
- Demeulemeester H, Vandesande F, Orban GA, Heizmann GW, Pochet R. 1989. Calbindin D-28K and parvalbumin are confined to two separate neuronal subpopulations in the cat visual cortex, whereas partial coexistence is shown in the dorsal lateral geniculate nucleus. *Neurosci Lett* 99:6–11.
- Fairén A, DeFelipe J, Regidor J. 1984. Nonpyramidal neurons: general account. In: Peters A, Jones EG, editors. *Cerebral cortex: cellular components of the cerebral cortex*. vol. 1. New York: Plenum Press. 201–253.
- Fonseca M, Del Río JA, Martínez A, Gómez S, Soriano E. 1995. Development of calretinin immunoreactivity in the neocortex of the rat. *J Comp Neurol* 361:177–192.
- Friauf E. 1994. Distribution of calcium-binding protein calbindin-D<sub>28k</sub> in the auditory system of adult and developing rats. *J Comp Neurol* 349:193–211.
- Gao W-J, Newman DE, Wormington AB, Pallas SL. 1999. Development of inhibitory circuitry in visual and auditory cortex of postnatal ferrets: Immunocytochemical localization of GABAergic neurons. *J Comp Neurol* 409:261–273.
- Gonchar Y, Burkhalter A. 1997. Three distinct families of GABAergic neurons in rat visual cortex. *Cereb Cortex* 7:347–358.
- Gordon-Weeks PR, Lockerbie RO, Pearce BR. 1984. Uptake and release of [<sup>3</sup>H]GABA by growth cones isolated from neonatal rat brain. *Neurosci Lett* 52:205–210.
- Guillery RW, Herrup K. 1997. Quantification without pontification: choosing a method for counting objects in sectioned tissues. *J Comp Neurol* 386:2–7.
- Hendrickson AE, van Brederode JFM, Mulligan KA, Celio MR. 1991. Development of the calcium-binding proteins parvalbumin and calbindin in monkey striate cortex. *J Comp Neurol* 307:626–646.
- Hendry SHC, Carder R. 1992. Organization and plasticity of GABA neurons and receptors in monkey visual cortex. In: Mize RR, Marc R, Sillito A, editors. *GABA in the retina and central visual system*. *Prog Brain Res* 90:477–502.
- Hendry SHC, Jones EG. 1991. GABA neuronal subpopulations in cat primary auditory cortex: co-localization with calcium binding proteins. *Brain Res* 543:45–55.
- Hendry SHC, Jones EG, Emson OC, Lawson DEM, Heizmann CW, Streit P. 1989. Two classes of cortical GABA neurons defined by differential calcium binding protein immunoreactivities. *Exp Brain Res* 76:467–472.
- Hensch T, Fagiolini M, Mataga N, Stryker M, Baekkeskov S, Kash S. 1998. Local GABA circuit control of experience-dependent plasticity in developing visual cortex. *Science* 282:1504–1508.
- Hof PR, Glezer II, Conde F, Flagg RA, Rubin MB, Nimchinsky EA, Vogt Weisenhorn DM. 1999. Cellular distribution of the calcium-binding proteins parvalbumin, calbindin, and calretinin in the neocortex of mammals: phylogenetic and developmental patterns. *J Chem Neuroanat* 16:77–116.

- Hogan D, Berman NEJ. 1993. Transient expression of calbindin-D28k immunoreactivity in layer V pyramidal neurons during postnatal development of kitten cortical areas. *Brain Res Dev Brain Res* 74:177–192.
- Hogan D, Berman NEJ. 1994. The development of parvalbumin and calbindin-D28k immunoreactive interneurons in kitten visual cortical areas. *Brain Res Dev Brain Res* 77:1–21.
- Hogan D, Terwilliger ER, Berman NEJ. 1992. Development of subpopulations of GABAergic neurons in cat visual cortical areas. *Neuroreport* 3:1069–1072.
- Huntley GW, Jones EG. 1990. Cajal-Retzius neurons in developing monkey cortex show immunoreactivity for calcium binding proteins. *J Neurocytol* 19:200–212.
- Issa NP, Trachtenberg JT, Chapman B, Zahs KR, Stryker MP. 1999. The critical period for ocular dominance plasticity in the ferret's visual cortex. *J Neurosci* 19:6965–6978.
- Jackson CA, Peduzzi JD, Hickey TL. 1989. Visual cortex development in the ferret. I. Genesis and migration of visual cortical neurons. *J Neurosci* 9:1242–1253.
- Jones EG, Hendryk SHC. 1984. Basket cells. In: Peters A, Jones EG, editors. *Cerebral cortex*, vol 1. New York: Plenum Press. p 309–336.
- Kelly JB, Judge PW, Phillips DP. 1986. Representation of the cochlea in primary auditory cortex of the ferret (*Mustela putorius*). *Hearing Res* 24:111–115.
- Kondo H, Hashikawa T, Tanaka K, Jones EG. 1994. Neurochemical gradient along the monkey occipito-temporal cortical pathway. *Neuroreport* 5:613–616.
- Lauder JM. 1993. Neurotransmitters as growth regulatory signals: role of receptors and second messengers. *Trends Neurosci* 16:233–240.
- Letinic K, Kostovic I. 1998. Postnatal development of calcium-binding proteins calbindin and parvalbumin in human visual cortex. *Cereb Cortex* 8:660–669.
- LoTurco JJ, Owens DF, Heath MJS, Davis MBE, Kriegstein AR. 1995. GABA and glutamate depolarize cortical progenitor cells and inhibit DNA synthesis. *Neuron* 15:1287–1298.
- Luskin MB, Shatz CJ. 1985a. Neurogenesis of the cat's primary visual cortex. *J Comp Neurol* 242:611–631.
- Luskin MB, Shatz CJ. 1985b. Studies of the earliest generated cells of the cat's visual cortex: cogeneration of subplate and marginal zones. *J Neurosci* 5:1062–1075.
- Marin-Padilla M. 1988. Early ontogenesis of the human cerebral cortex. In: Peters A, Jones EG, editors. *Cerebral cortex*. Vol 7, Development and maturation of cerebral cortex. New York: Plenum. p 1–33.
- Marin-Padilla M. 1998. Cajal-Retzius cells and the development of the neocortex. *Trends Neurosci* 21:64.
- McBurney RN, Neering IR. 1987. Neuronal calcium homeostasis. *Trends Neurosci* 10:164–169.
- McConnell SK. 1985. Migration and differentiation of cerebral cortical neurons after transplantation into the brains of ferrets. *Science* 229:1268–1271.
- McMullen NT, Smelser CB, de Venecia RK. 1994. A quantitative analysis of parvalbumin neurons in rabbit auditory neocortex. *J Comp Neurol* 349:493–511.
- Moore DR, Hine JE. 1992. Rapid development of the auditory brainstem response threshold in individual ferrets. *Brain Res Dev Brain Res* 66:229–235.
- Newman DE, Gonzalez H, Wormington A, Pallas SL. 1996. Postnatal development of GABA, parvalbumin, and calbindin immunoreactivity in ferret visual and auditory cortex. *Soc Neurosci Abstr* 22:1973.
- Owens DF, Boyce LH, Davis MBE, Kriegstein AR. 1996. Excitatory GABA responses in embryonic and neonatal cortical slices demonstrated by gramicidin perforated-patch recordings and calcium imaging. *J Neurosci* 16:6414–6423.
- Pallas SL, Gilmour SM, Finlay BL. 1988. Control of cell number in the developing neocortex. I. Effects of early tectal ablation. *Brain Res Dev Brain Res* 43:1–11.
- Peters A. 1984. Chandelier cells. In: Peters A, Jones EG, editors. *Cerebral cortex*, vol 1. New York: Plenum Press. p 361–379.
- Peters A, Jones EG. 1984. *Cerebral cortex*. Vol 1, Cellular components of the cerebral cortex. New York: Plenum Press.
- Popken GJ, Farel PB. 1996. Reliability and validity of the physical disector method for estimating neuron number. *J Neurobiol* 31:166–174.
- Preuss TM, Kaas JH. 1996. Parvalbumin-like immunoreactivity of layer V pyramidal cells in the motor and somatosensory cortex of adult primates. *Brain Res* 712:353–357.
- Rakic P. 1974. Neurons in the rhesus monkey visual cortex: systematic relation between time of origin and eventual disposition. *Science* 183:425–427.
- Reiter HO, Stryker MP. 1988. Neural plasticity without postsynaptic action potentials: less-active inputs become dominant when kitten visual cortical cells are pharmacologically inhibited. *Proc Natl Acad Sci USA* 85:3623–3627.
- Rose JE. 1949. The cellular structure of the auditory region of the cat. *J Comp Neurol* 91:408–440.
- Ruthazer ES, Baker GE, Stryker MP. 1999. Development and organization of ocular dominance bands in primary visual cortex of the sable ferret. *J Comp Neurol* 407:151–165.
- Rutherford LC, DeWan A, Lauer HM, Turrigiano GG. 1997. Brain-derived neurotrophic factor mediates the activity-dependent regulation of inhibition in neocortical cultures. *J Neurosci* 17:4527–4535.
- Sato H, Katsuyama N, Tamura H, Hata Y, Tsumoto T. 1995. Mechanisms underlying direction selectivity of neurons in the primary visual cortex of the macaque. *J Neurophysiol* 74:1382–1394.
- Sato H, Katsuyama N, Tamura H, Hata Y, Tsumoto T. 1996. Mechanisms underlying orientation selectivity of neurons in the primary visual cortex of the macaque. *J Physiol (Lond)* 494:757–771.
- Sillito AM. 1975a. The contribution of inhibitory mechanisms to the receptive field properties of neurones in the striate cortex of the cat. *J Physiol (Lond)* 250:305–329.
- Sillito AM. 1975b. The effectiveness of bicuculline as an antagonist of GABA and visually evoked inhibition in the cat's striate cortex. *J Physiol (Lond)* 250:287–304.
- Sokal RR, Rohlf FJ. 1995. *Biometry*. New York: W.H. Freeman.
- Stichel CC, Singer W, Heizmann CW, Norman AW. 1987. Immunohistochemical localization of calcium-binding proteins, parvalbumin and calbindin D-28K, in the adult and developing visual cortex of cats: a light and electron microscopic study. *J Comp Neurol* 262:563–577.
- Tago H, McGeer P, McGeer E, Akiyama H, Hersh L. 1989. Distribution of choline acetyltransferase immunopositive structures in the rat brainstem. *Brain Res* 495:271–297.
- van Brederode JFM, Mulligan KA, Hendrickson AE. 1990. Calcium-binding proteins as markers for subpopulations of GABAergic neurons in monkey striate cortex. *J Comp Neurol* 298:1–22.
- van Brederode JFM, Helliesen MK, Hendrickson AE. 1991. Distribution of the calcium-binding proteins parvalbumin and calbindin-D28k in the sensorimotor cortex of the rat. *Neuroscience* 44:157–171.
- Vogt Weisenhorn DM, Celio MR, Rickmann M. 1998. The onset of parvalbumin-expression in interneurons of the rat parietal cortex depends upon extrinsic factor(s). *Eur J Neurosci* 10:1027–1036.
- Yan XX, Cao QL, Luo XG, Garey LJ. 1997. Prenatal development of calbindin D-28K in human visual cortex. *Cereb Cortex* 7:57–62.
- Yan YH, van Brederode JFM, Hendrickson AE. 1995a. Developmental changes in calretinin expression in GABAergic and nonGABAergic neurons in monkey striate cortex. *J Comp Neurol* 363:78–92.
- Yan YH, van Brederode JFM, Hendrickson AE. 1995b. Transient colocalization of calretinin, parvalbumin, and calbindin-D28K in developing visual cortex of monkey. *J Neurocytol* 24:825–837.
- Yuste R, Katz LC. 1991. Control of postsynaptic Ca<sup>2+</sup> influx in developing neocortex by excitatory and inhibitory neurotransmitters. *Neuron* 6:333–344.
- Zheng W, Knudsen E. 1999. Functional selection of adaptive auditory space map by GABA<sub>A</sub>-mediated inhibition. *Science* 284:962–965.